Le changement de phase liquide ➔ solide

Charles-André GANDIN

MINES ParisTech CEMEF UMR CNRS 7635
06904 Sophia Antipolis, France

Action Nationale de Formation « METALLURGIE FONDAMENTALE »
22-25 octobre 2012, Aussois, France

Statistics

- Alloys are produced by primary melting and transformed by secondary melting, thus involving the liquid-to-solid phase transformation
- Primary production of alloys in 2010

	Fe	Al	Cu	Zn	Pb	Ni	Sn
World (Mtons)	1'518	40.4	14.6	12.9	8.8	1.4	0.3
France (Mtons)	15.8	0.421	0.428	0.163	0.088	0.107	-
France (people)	23'800	3'594	3'600	-	-	4'300	-

www.societechimiquedefrance.fr

- Solidification is part of metallurgy textbooks
  - "Métallurgie: du minerai au matériau", J. PHILIBERT, A. VIGNES, Y. BRÉCHET, P. COMBRADE, Dunod (Paris, FR) 2002.
  - "Solidification", J. A. DANTZIG, M. RAPPAZ, EPFL Press (Lausanne, CH) 2009.

www.solidification.org

Statistics

- Laboratories/People in France
  - GdR CNRS 3328 « Solidification des Alliages Métalliques » (COMBEAU)
    - « Formation des microstructures » (BILLIA, AKAMATSU, LACAZE, DALOZ)
    - « Dynamique de la zone pâteuse » (RAPPAZ, ZALOZNIK, SUERY)
    - « Procédés » (GANDIN, FAUTRELLE, DREZET, PEYRE, BIGOT, DUFFAR)

Laboratory	People	Section CN	Laboratory	People	Section CN
IJL, Nancy	4	15	CEMEF, Sophia Antipolis	3	9, 15
CIRIMAT, Toulouse	2	15	CDM, Evry	1	9, 15
SIMAP, Grenoble	4	15 (9,10)	PIMM, Paris	5	9, 10
ICMB, Bordeaux	4	15, 10	LCFC, Metz	3	9
ICB, Dijon	4	14, 15	LMGC, Montpellier	3	9
EM2C, Châtenay-Malabry	2	10	IM2NP, Marseille	7	5, 15
TREFLE, Pessac	2	10	INSP, Paris	3	5
IRPHE, Marseille	3	10	LPMC, Palaiseau	2	5
LSMX, Lausanne, CH	*3*		CEA-INES, Le Bourget-du-Lac	6	

http://spinonline.free.fr/GDR

- Commission SF2M « Coulée et Solidification » (JARRY)

Processes

- Semi-finished products
  - continuous, semi-continuous, ingots (casting)

CC of steel

semi-CC of aluminum

ingot casting of steel

- Near-net-shape products
  - expendable: sand, plaster, shell, plaster, investment , loast foam (casting)
  - non-expendable: centrifugal, semi-solid, die, permanent mold (casting)

sand casting of steel

cast engine block

- Assembly
  - welding (TIG, MIG, MAG, laser, …)
  - soldering, brazing

tungsten inert gas welding

investment shell

cast turbocharger rotor

Defects

- Part integrity (cracks, misruns, …)
- Structure selection (columnar, equiaxed, dendritic, eutectic, …)
- Phase selection (nature and size)
- Crystallographic texture (fiber)
- Segregation (inverse, buoyancy forces, grain sedimentation, inter-granular, interdendritic, freckles, …)
- Porosity (hot spot, shrinkage, gas)
- Residual stresses
- Hot tears

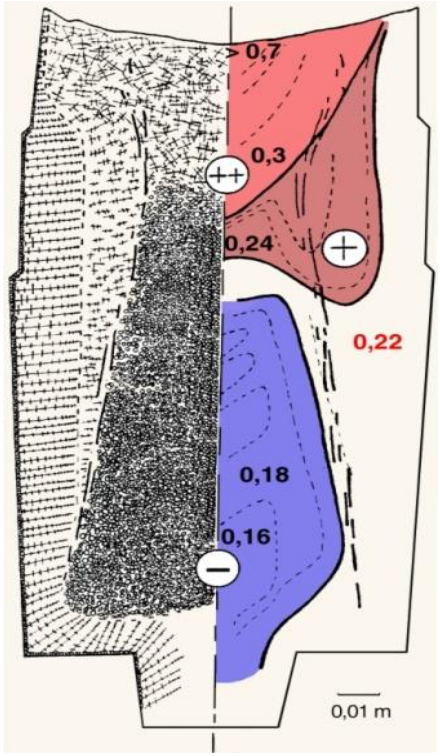

segregation map in forge ingot

cold crack in semi-CC of aluminum

stray grain in a “single crystal” turbine blade

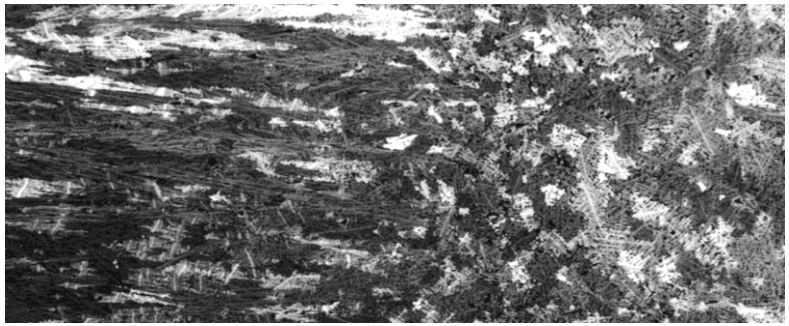
columnar-to-equiaxed transition

hot tear in weld

Structures

- Structures formed from a binary melt
  - dendritic, $l_1 \rightarrow \alpha + l_2$ (monovariant reaction),
  - peritectic, $l + \alpha \rightarrow \beta$ (invariant reaction),
  - eutectic, $l \rightarrow \alpha + \beta$ (invariant reaction),
  - congruent, $l \rightarrow \alpha$ (invariant reaction),
  - monotectic, $l_1 \rightarrow l_2 + \alpha$ (invariant reaction).
- Selection and fraction of structures and phases are influenced by
  - alloy composition (industrial = multicomponent),
  - departure from thermodynamic equilibrium (nucleation and growth undercooling),
  - diffusion in phases (with $D^s << D^l$),
  - phase flow (melt and solid),
  - heat flow (temperature gradient, isotherm velocity).

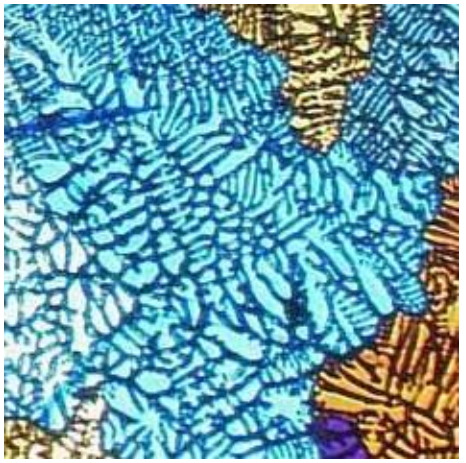

Dendritic
(cast AlMgFeSi)

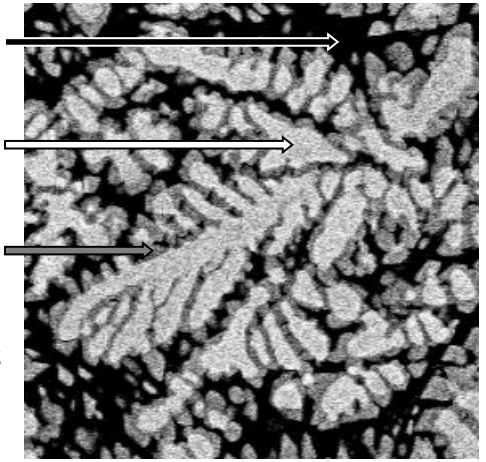

Peritectic
(atomized NiAl)

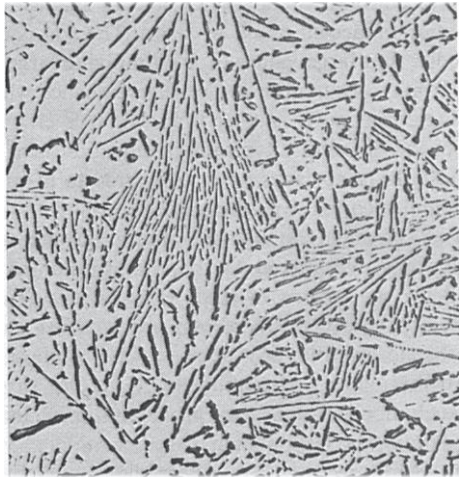

Eutectic
(cast AlSi)

Segregations

- Segregations form due to
  - thermodynamic equilibrium between phases with different solubility of species, defined by the segregation coefficient $k=(X^s/X^l)_{T,p}$
- Main outputs of segregation studies
  - composition profile and average composition of phases,
  - fraction of structures and phases,
  - fraction of phases in each structure,
  - solidification path (above information as a function of temperature from T_L to T_S)
- Simple examples of solidification paths, with common assumption a uniform liquid composition ($D^l>>0$)
  - Lever Rule (LR): equal chemical potentials of all species in all phases ($D^s>>0$)
  - Gulliver-Scheil (GS): same as LR at the s/l interface with $D^s=0$
  - Partial Equilibrium (PE): mixture of GS for substitutionals and LR for interstitials

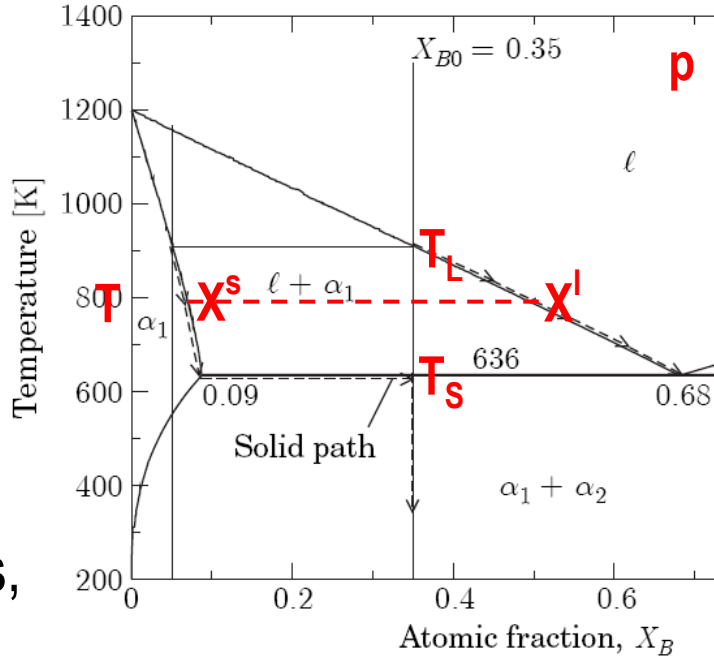

Scales

Atom Probe Tomography

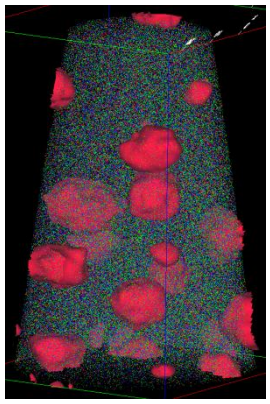

Electron microscopy

Optical microscopy

Casting

Observations

Molecular dynamics

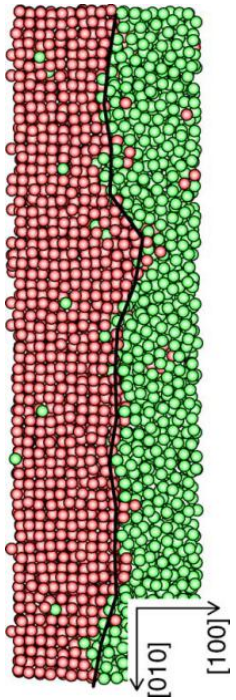

Phase field

Cellular automaton

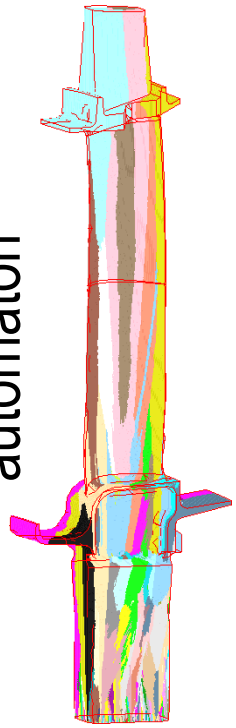

Continuum mechanics

Simulations

10^{-9} 10^{-6} 10^{-3} 1 m

10^{-12} 10^{-8} 10^{-4} 1 10^{4} s

Methodologies

Scales \ Methods	Indirect	Direct
Macroscopic	**Volume averaging over a multiphase domain** 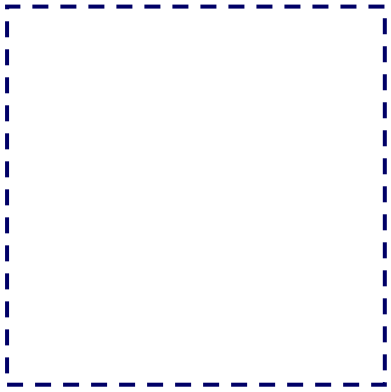 *Solidification paths* Continuum mechanics	**Tracking of domain boundaries** 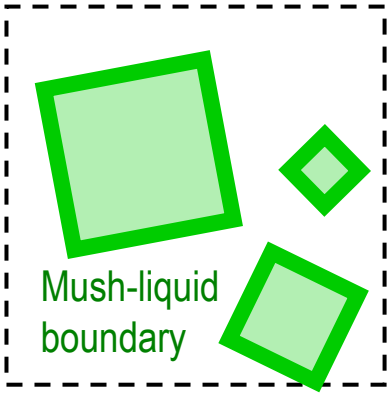 *Solidification paths* *Interface kinetics* Structure kinetics for the prediction of grain size distribution Mush-liquid boundary
Grain Microscopic	**Volume averaging over each independent phase** 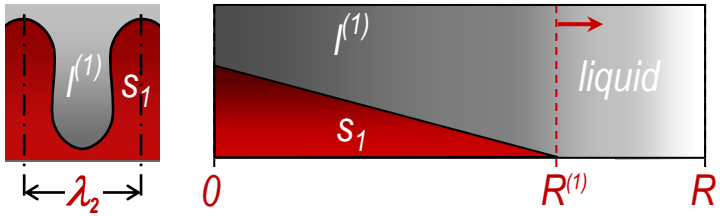 Solidification paths and interface kinetics for the prediction of average phase fractions and compositions	**Tracking of phase interfaces** 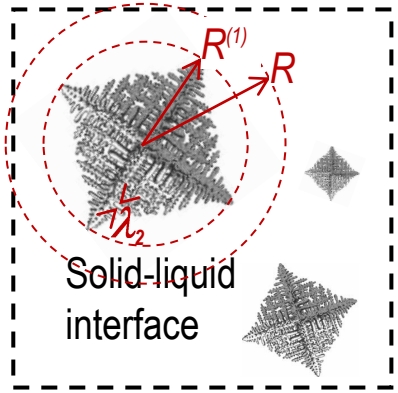 Diffuse interface for the prediction of microstructure Solid-liquid interface

Contents

- Introduction
  - Statistics, Processes & Defects
  - Structures & Segregations
  - Scales & Methodologies
- Direct microscopic methodology
- Indirect microscopic methodology
  - Observations: electromagnetic levitation and atomization
  - Kinetics modeling coupled with equilibrium calculations
  - Applications and current extensions
- Indirect macroscopic methodology
  - Phase field modeling of microstructures
- Direct macroscopic methodology
  - CAFE modeling
  - Application to ESRF observations
  - Application to directionally solidified grain structure
  - Application to a macrosegregation benchmark experiment
- Perspectives

Direct microscopic methodology

- The phase field method tracks to phase interfaces
- Applications to solidification include quantitative studies on structure dynamics (PLAPP, Ecole Polytechnique, Palaiseau)

www.solidification.org

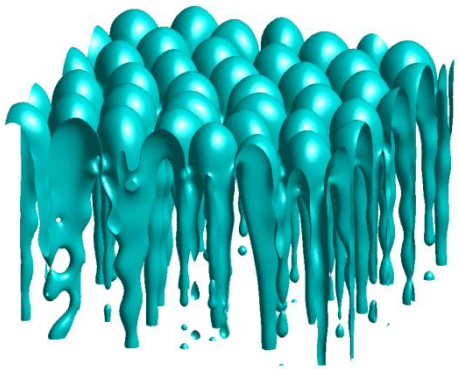

Directional solidification in a dilute alloy

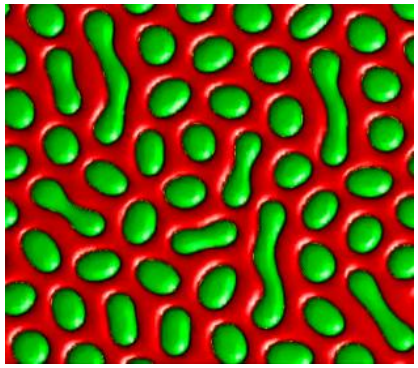

Non-faceted eutectic structure

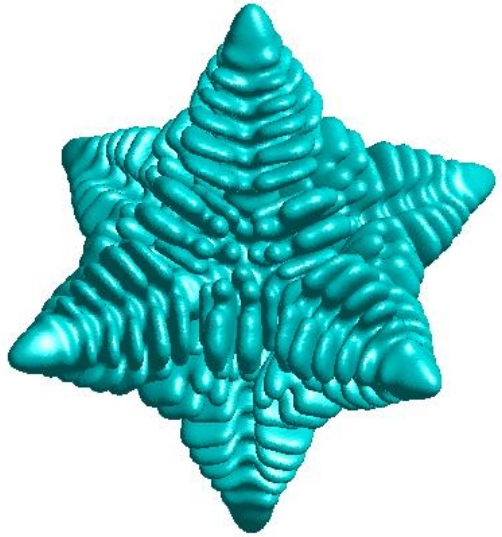

Equiaxed solidification in pure substance

- Most developed models consider multicomponent alloys and multiple phase transformations coupled with thermodynamic databases (Code MICRESS, ACCESS, Aachen, DE)

Limits of interface tracking

- Biggest phase field result for a network of dendrites in Al-Si?

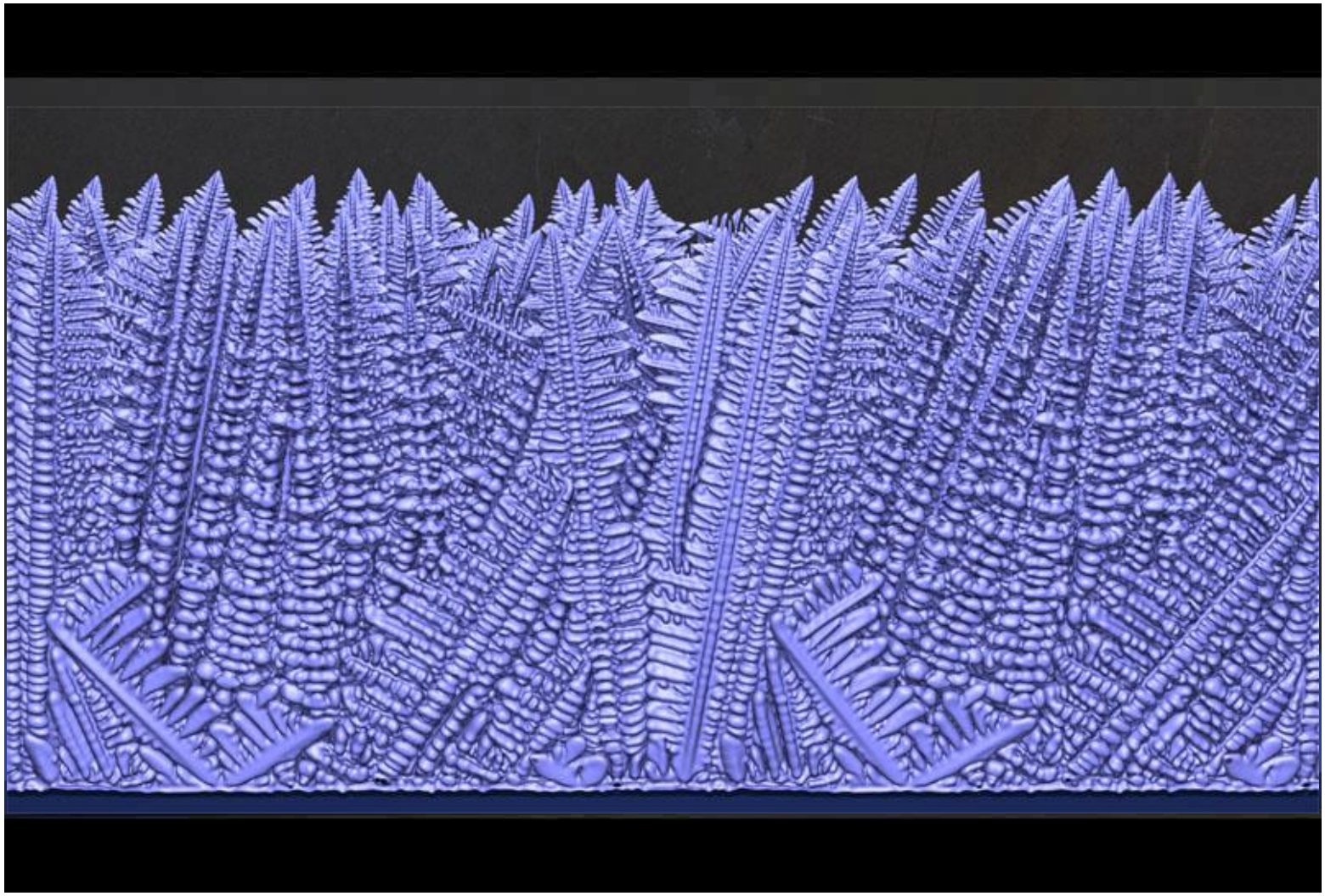

Size is given by the number of grid point: 4096x1024x4096 **(only few cubic millimeters!)**

Parallel computation with up to 4'000 GPUs and 16'000 CPUs, reaching 2 petaFLOPS

GPU = Graphics Processing Unit, CPU = Central Processing Units, petaFLOPS = 10^{15} FLoating point Operations Per Seconds

T. Shimokawabe, T. Aoki, T. Takaki, A. Yamanaka, A. Nukada, T. Endo, N. Maruyama, S. Matsuoka, Proceedings of the 2011 ACM/IEEE International Conference for High Performance Computing, Networking, Storage and Analysis, SC'11, IEEE Computer Society, Seattle, WA, USA, Nov. 2011.

Indirect microscopic methodology

- Collaborations
  - D. TOURRET, MINES ParisTech, Sophia Antipolis
  - D. HERLACH, Th. VOLKMANN, D. TOURRET, DLR, Köln, DE
  - M. CALVO-DAHLBORG, U. DAHLBORG, C. M. BAO, University, Rouen
  - G. REINHART, University Paul Cézanne, Marseille,
  - G. N. ILES, ESRF/ILL, Grenoble
- Funding
  - European Community, Brussels, BE
  - European Space Agency, Noordwijk, NL
  - Bundesvereinigung Materialwissenschaft und Werkstofftechnik e.V., Berlin, DE
  - Deutsche Forschungsgemeinschaft, Bonn, DE
  - Bundesanstalt für Materialforschung und –prüfung, Berlin, DE

Tourret et al., Acta mater. 2009 57 2066, Acta mater. 2011 59 4665, Acta mater. 2011 59 6658

Observations

Indirect micro

- Gas atomization of Al-Ni alloys

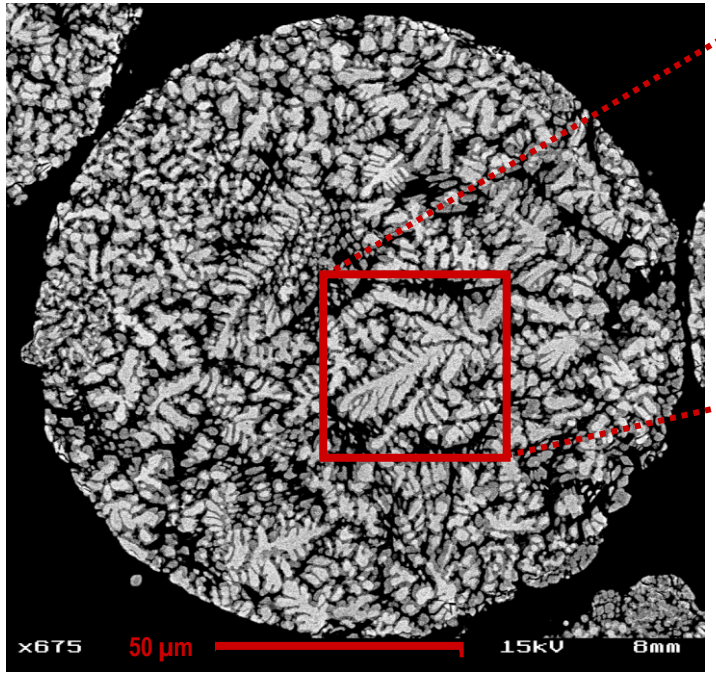

SEM image of a Ni-75at% Al 100 μm diameter droplet produced by gas atomization

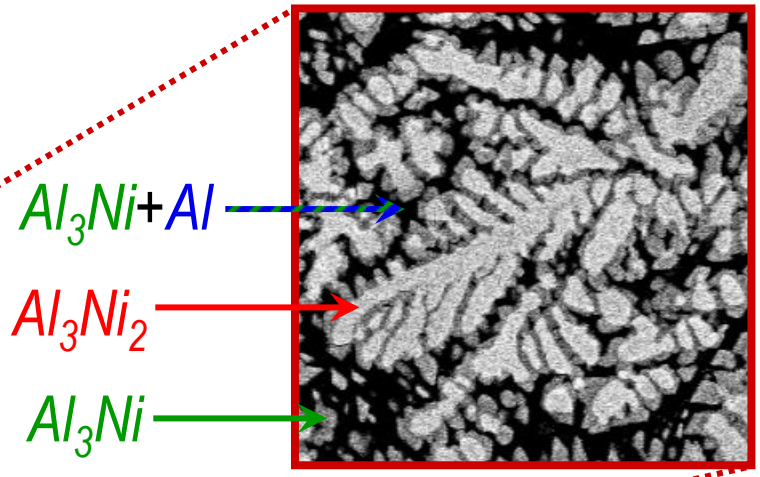

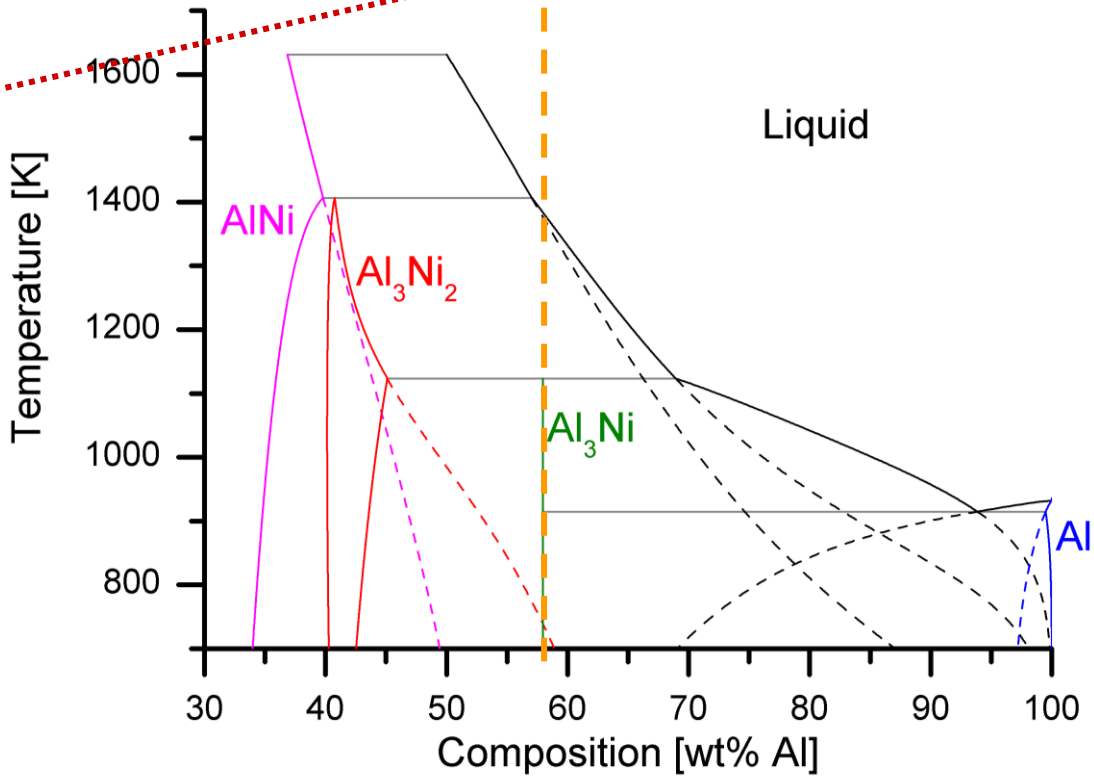

- Concurrent multiple phase transformations

(Rappaz&Thévoz 1987, Wang&Beckermann 1993, Appolaire et al. 2008)

- Constant and equal density in all phases
- Uniform T with heat exchange rate Q
- Zones & phases defined by boundaries & interfaces
  - (0): $l^{(0)}$ (1): $s_1^{(1)}+l^{(1)}$
  - (2): $s_1^{(2)}+s_2^{(2)}+l^{(2)}$
  - (3): $s_1^{(3)}+s_2^{(3)}+s_3^{(3)}$
- Microstructure propagation at zone boundaries with growth kinetics
  - s_1: dendritic
  - s_2: peritectic
  - s_3: eutectic
- Thermodynamic equilibrium at phase interfaces
- Unknowns: average composition and phase fractions
  - $l^{(0)}$ $l^{(1)}$ $s_1^{(1)}$
  - $l^{(2)}$ $s_1^{(2)}$ $s_2^{(2)}$
  - $s_1^{(3)}$ $s_2^{(3)}$ $s_3^{(3)}$

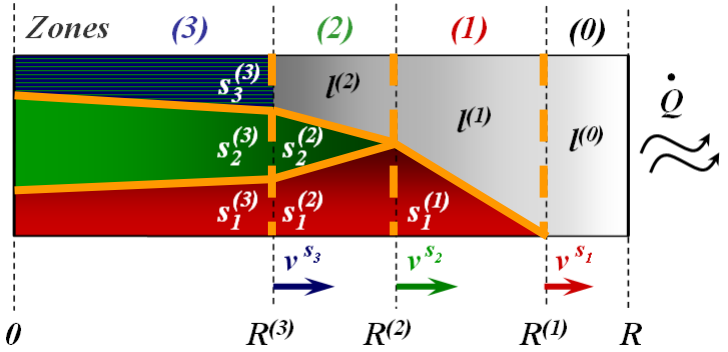

Modeling — Indirect micro

- **Average total mass**

over phase (α) : $$\frac{\partial}{\partial t}\left(g^{\alpha}\right) = \sum_{\beta\ (\beta\neq\alpha)} \left(S^{\alpha\beta}\, v_n^{\alpha\beta}\right)$$

on interface ($\alpha\beta$) : $$v_n^{\alpha\beta} + v_n^{\beta\alpha} = 0$$

- **Average solute mass**

over phase (α) : $$g^{\alpha}\frac{\partial}{\partial t}\left(\langle w^{\alpha}\rangle^{\alpha}\right) = \sum_{\beta\ (\beta\neq\alpha)} \left[S^{\alpha\beta}\left(w^{\alpha\beta} - \langle w^{\alpha}\rangle^{\alpha}\right)\left(v_n^{\alpha\beta} + \frac{D^{\alpha}}{l^{\alpha\beta}}\right)\right]$$

on interface ($\alpha\beta$) : $$\left(w^{\alpha\beta} - w^{\beta\alpha}\right) v_n^{\alpha\beta} + \frac{D^{\alpha}}{l^{\alpha\beta}}\left(w^{\alpha\beta} - \langle w^{\alpha}\rangle^{\alpha}\right) + \frac{D^{\beta}}{l^{\beta\alpha}}\left(w^{\beta\alpha} - \langle w^{\beta}\rangle^{\beta}\right) = 0$$

- **Average energy balance**

Global heat balance: $$\rho\frac{\partial \langle H\rangle}{\partial t} = \rho\sum_{\alpha}\left(\langle H^{\alpha}\rangle^{\alpha}\frac{\partial g^{\alpha}}{\partial t} + g^{\alpha}\frac{\partial \langle H^{\alpha}\rangle^{\alpha}}{\partial T}\frac{\partial T}{\partial t} + g^{\alpha}\frac{\partial \langle H^{\alpha}\rangle^{\alpha}}{\partial \langle w^{\alpha}\rangle^{\alpha}}\frac{\partial \langle w^{\alpha}\rangle^{\alpha}}{\partial t}\right) = -h_c\, S^{ext}\left(T - T_{ext}\right)$$

- **Additional relations and Unknowns**

Geometry & Composition profiles assumptions: $S^{\alpha\beta}$, $l^{\alpha\beta}$, S^{ext}

Boundary conditions: h_c, Text Data: D^{α}, $\Delta T_n^{s\alpha}$

Thermodynamic equilibrium: $\langle H^{\alpha}\rangle^{\alpha}$, $\partial\langle H^{\alpha}\rangle^{\alpha}/\partial T$, $\partial\langle H^{\alpha}\rangle^{\alpha}/\partial\langle w^{\alpha}\rangle^{\alpha}$ ← ThermoCalc+Database

Interface: Equilibrium: $w^{\alpha\beta}$ ← Boundary: Growth kinetics: $v_n^{\alpha\beta}$

Solute balance: $v_n^{\alpha\beta}$ Solute balance & Continuity: $w^{\alpha\beta}$

Partial Derivative Equations: g^{α}, $\langle w^{\alpha}\rangle^{\alpha}$, T

Electromagnetic levitation

Indirect micro

- Containerless processing
  - Controlled conditions, almost uniform temperature, observation of nucleation events
- Droplet: benchmark system for volume averaged models
  - Gandin et al. 2008, Acta mater. 56 3023, Heringer et al. 2006, Acta mater. 54 4427

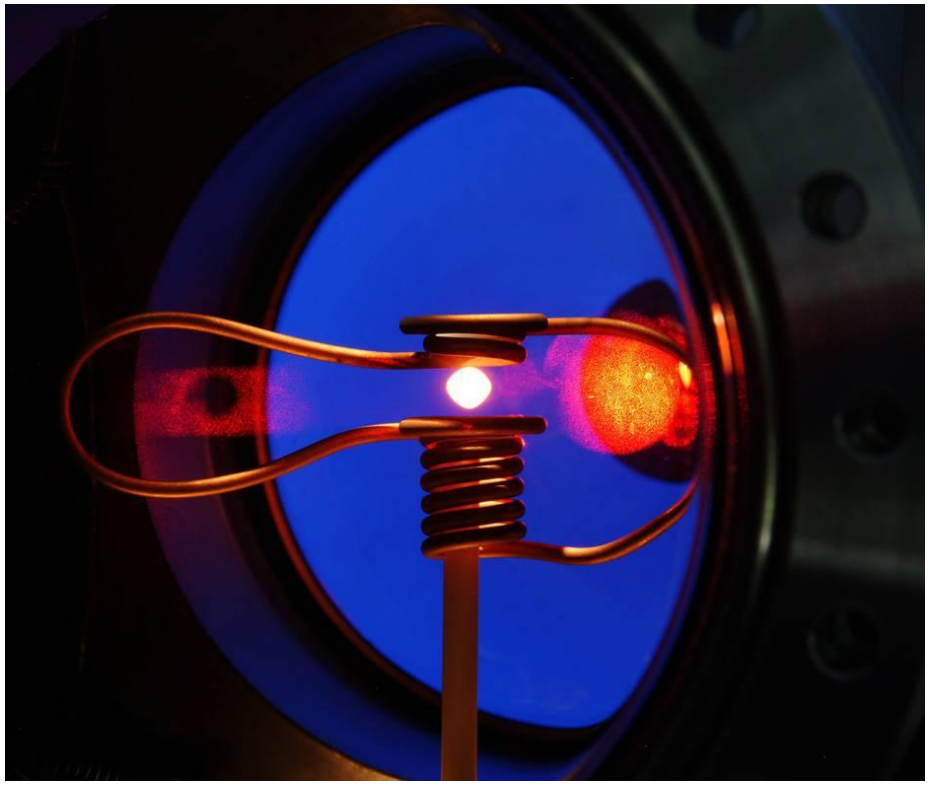

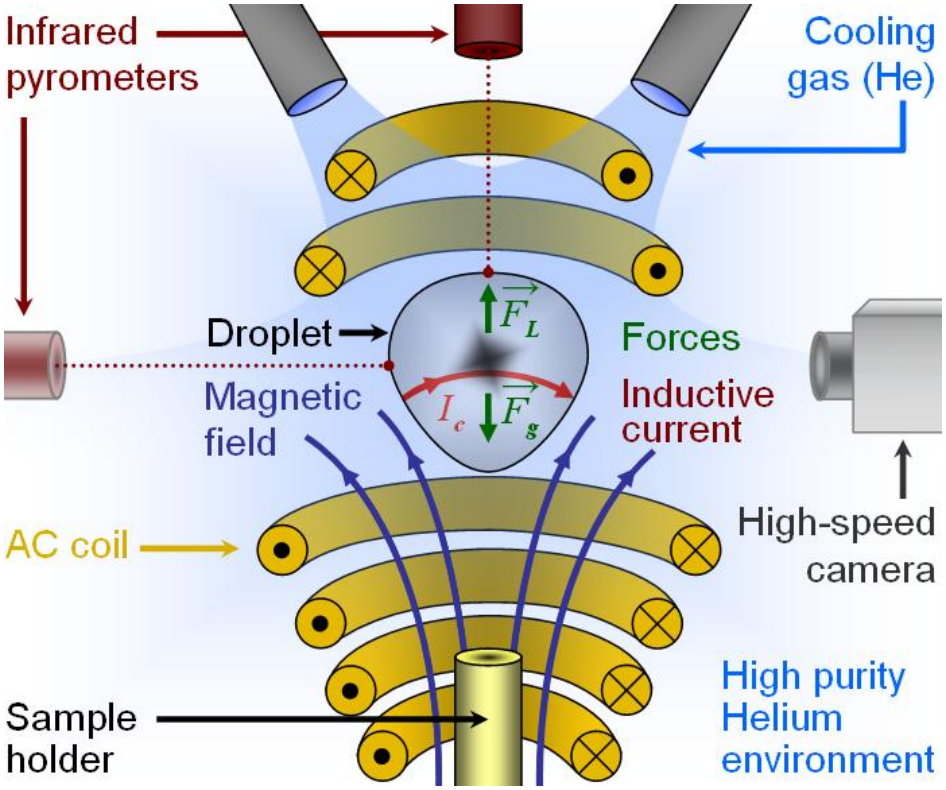

Electromagnetic levitation — Indirect micro

- Alloy — Ni - 75 at% Al
- Thermodynamic database — PBIN
- System radius [d] — $3.82 \cdot 10^{-3}$ m
- Dendrite arm spacing [d] — $36 \cdot 10^{-6}$ m
- Diffusion coefficients
  - Liquid — 10^{-9} m^2 s^{-1}
  - Al_3Ni_2, Al_3Ni — $5 \cdot 10^{-11}$ m^2 s^{-1}
- Gibbs-Thomson coefficients
  - Al_3Ni_2 — $2 \cdot 10^{-8}$ K m
  - Al_3Ni [M] — $3.5 \cdot 10^{-8}$ K m
  - Al [M] — $1.86 \cdot 10^{-7}$ K m
- Nucleation undercooling
  - Al_3Ni_2, Al_3Ni, Al [d] — 0 K, 150 K, 15 K
- Heat transfer [d] — 213.8 W m^{-2} K^{-1}
- External temperature [d] — 293 K

[d]: *deduced from measurements*

[M]: *Marasli&Hunt 1996 Acta Mater.*

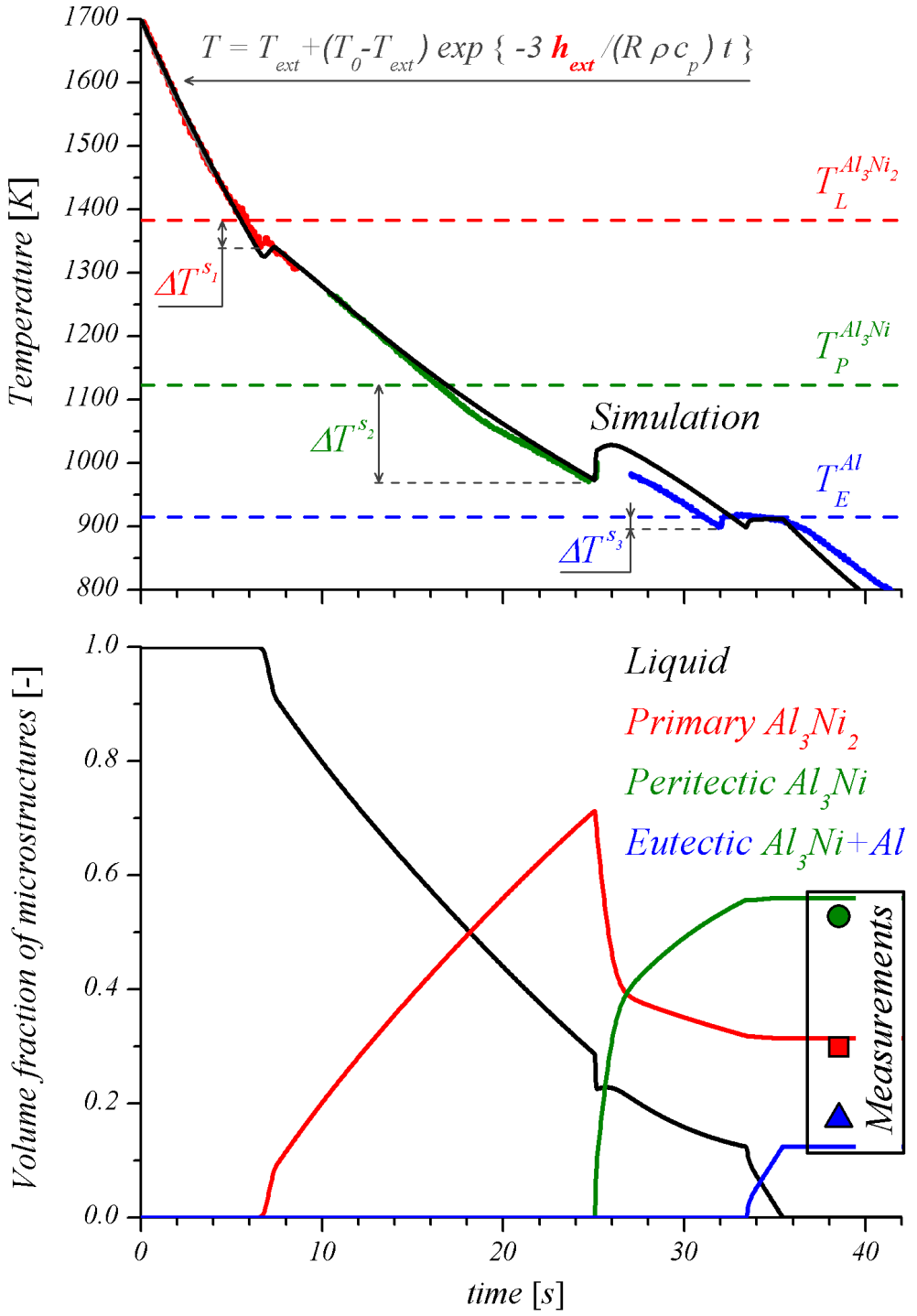

Atomization

Indirect micro

- *Regime I: Classical Fourier number analysis*

  The peritectic transformation controls the phase fractions due to diffusion in the solid phases. It is favored for lower cooling rates (larger particles).

- *Regime II: Al_3Ni primary growth*

  Primary growth of Al_3Ni controls the phase fraction. It prevents the development of Al_3Ni_2.

- *Regime III: Al_3Ni_2 and Al_3Ni growth competition*

  Mixed regime where the peritectic reaction for Al_3Ni can catch-up with the dendritic reaction of Al_3Ni_2 and become primary when the cooling rate is increased.

Evidence of growth competition between phases formed from the melt

Current extensions: multicomponent alloys (AM1), multiple phase transformations (FeCCr)

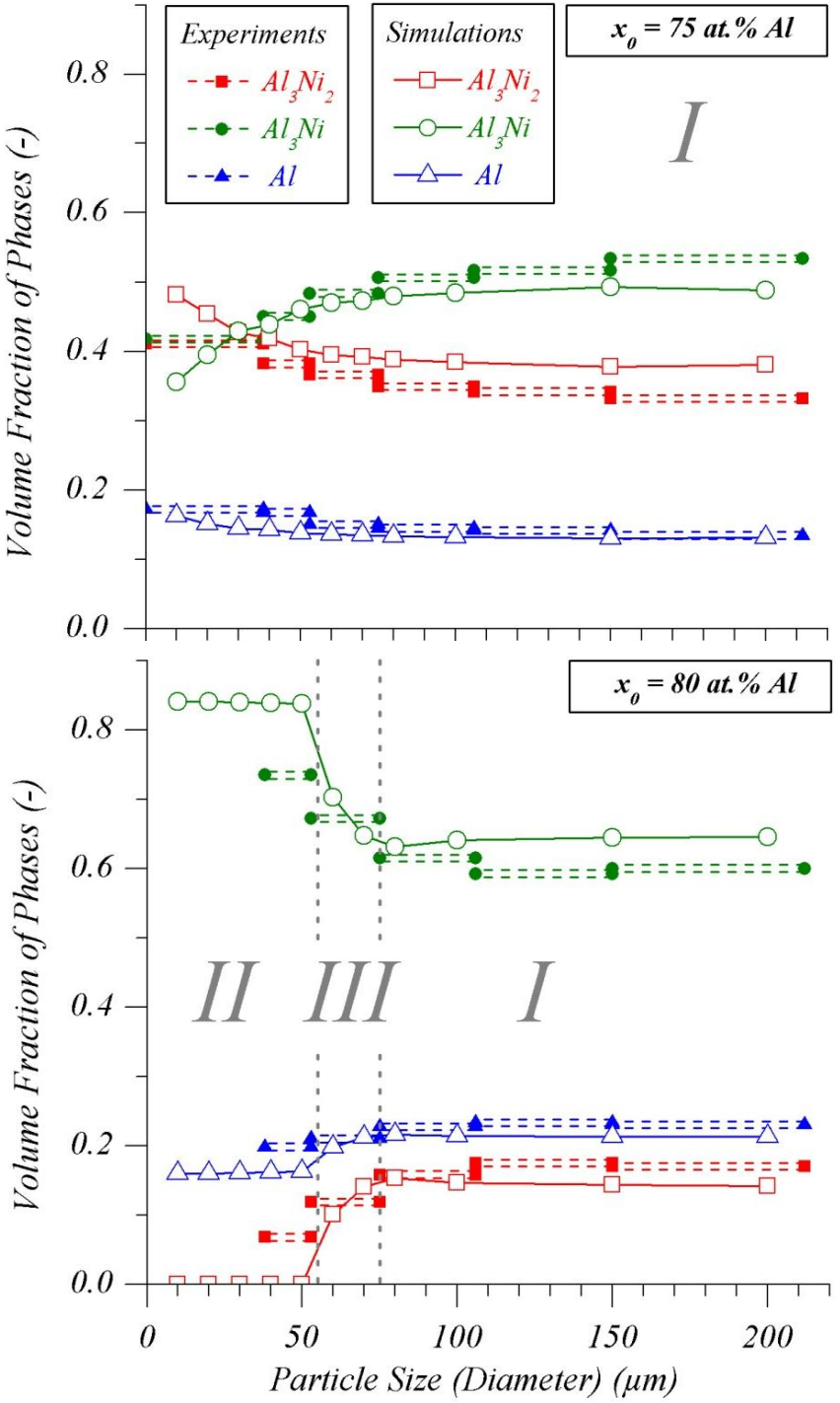

Direct macroscopic methodology

- Collaborations
  - T. CAROZZANI, M. BELLET, H. DIGONNET, MINES ParisTech, Sophia Antipolis
  - Y. FAUTRELLE, K. ZAIDAT, Institut National Polytechnique de Grenoble, Grenoble
  - G. REINHART, N. MANGELINCK-NOËL, H. NGUYEN-THI, B. BILLIA, Aix-Marseille Université, Marseille
  - J. BARUCHEL, ESRF, Grenoble

- Funding
  - European Space Agency, Noordwijk, NL
  - Agence Nationale de la Recherche, Paris

Indirect macroscopic methodology

Two-phase model assuming $\langle\rho\rangle^s=\langle\rho\rangle^l=\rho_0$=constant and $\langle\mathbf{v}\rangle^s=0$

Total mass conservation $\nabla\cdot\langle\mathbf{v}\rangle = 0$

Average flow velocity $\langle\mathbf{v}\rangle = \langle\mathbf{v}^l\rangle = g^l\,\langle\mathbf{v}\rangle^l$

Momentum conservation $$\rho_0\frac{\partial\langle\mathbf{v}^l\rangle}{\partial t} + \frac{\rho_0}{g^l}\nabla\cdot\left(\langle\mathbf{v}^l\rangle\times\langle\mathbf{v}^l\rangle\right) - \nabla\cdot\left(\mu^l\nabla\langle\mathbf{v}^l\rangle\right) + g^l\nabla p^l - g^l\rho\mathbf{g} + \frac{\mu^l}{K}g^l\langle\mathbf{v}^l\rangle = 0$$

Boussinesq approximation $\rho = \rho_0\left[1 - \beta_{th}\,(T - T_0) - \beta_w\,(w^l - w_0^l)\right]$

Carman-Kozeny permeability $K = \left(g^{l3}\,\lambda_2{}^2\right) / \left(180\,(1-g^l)^2\right)$

Energy conservation $$\rho_0\left(\frac{\partial\langle H\rangle}{\partial t} + \langle\mathbf{v}\rangle\cdot\nabla\langle H\rangle^l\right) - \nabla\cdot\left(\langle\kappa\rangle\,\nabla T\right) = 0$$

Average enthalpy $\langle H\rangle = g^s\,\langle H\rangle^s + g^l\,\langle H\rangle^l$

Solute mass conservation $$\frac{\partial\langle w\rangle}{\partial t} + \langle\mathbf{v}\rangle\cdot\nabla\langle w\rangle^l - \nabla\cdot\left(D^l\,g^l\,\nabla\langle w\rangle^l\right) = 0$$

Average composition $\langle w\rangle = g^s\,\langle w\rangle^s + g^l\,\langle w\rangle^l$

The FE method provides a solution for $\langle v\rangle$, $\langle H\rangle$, $\langle w\rangle$, T

G. Guillemot et al. 2007 Journal of Crystal Growth 303 58

Transport between scales

Direct macro

- A CA grid of square cells is superimposed on top of the FE mesh
- Topological links are defined between the FE nodes and the CA cells
- Quantity at cell ν, ξ_ν (e.g., $\langle v \rangle$, $\langle H \rangle$, $\langle w \rangle$, T), is computed from quantity at nodes n, ξ_n, thanks to interpolation coefficients c

$$\xi_\nu = \sum_n c_\nu^n \, \xi_n$$

- and oppositely,

$$\xi_n = \left(\sum_\nu c_\nu^n \, \xi_\nu \right) / \left(\sum_\nu c_\nu^n \right)$$

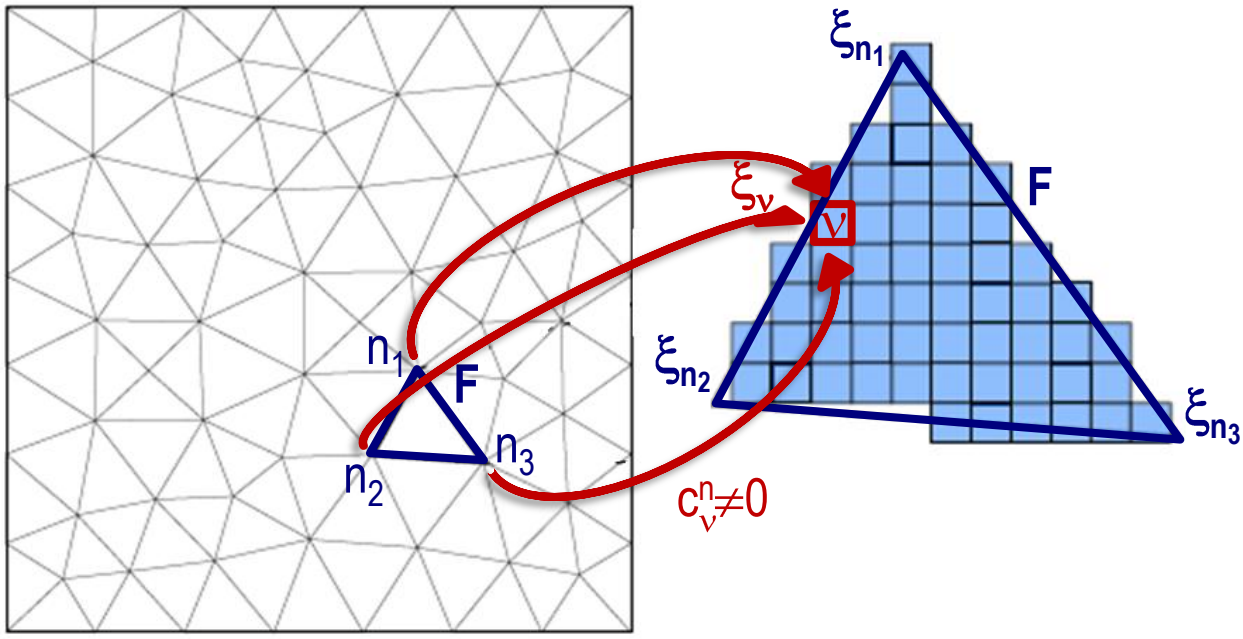

Carozzani et al. 2012 MSMSE 20 015010

Nucleation algorithm

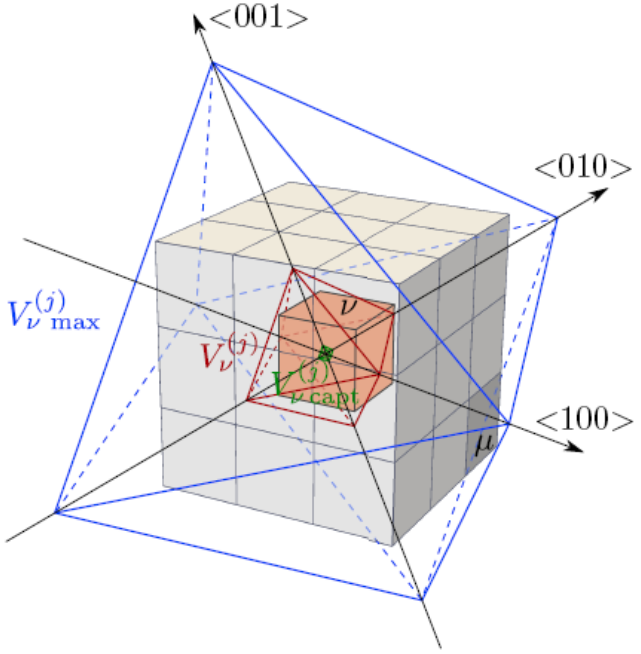

- State index of cell ν wrt structure (j), $I^{(j)}_{\nu}$
  - 0: no growing structure
  - 1: growing structure
  - 2: structure growth over
- Structure nucleation in cell ν
  - Test for $I^{(j)}_{\nu} = 0$ prior to nucleation, change to $I^{(j)}_{\nu} = 1$ after nucleation
  - Test for $\Delta T_{\nu} > \Delta T^{nucl(j)}_{\nu}$, the activation undercooling of the nucleation site of structure (j) located in cell ν (undercooling = temperature difference between the local liquidus temperature, T_L, and the actual cell temperature, T_{ν})
  - Initialization of a set of Euler angles $(\phi_1,\Phi,\phi_2)^{(j)}_{\nu}$ defining the 6 perpendicular <100> directions
  - Growth center $C^{(j)}_{\nu}$ coincides with cell center $C_{\nu 0}$
  - Initialization of the lengths of the preferred <100> growth directions $R^{(j)<100>}_{\nu}$ (for a <100> dendritic structure (j))

Growth algorithm

- Structure growth in cell ν
  - Increase of lengths $R^{(j)<100>}_{\nu}$ by time integration of a phenomenological dendrite tip growth kinetics model that depends on local temperature, T_{ν}, composition, $<w>_{\nu}$, and liquid velocity, $<\mathbf{v}>^{l}_{\nu}$
  - Calculation of volume associated with the growth shape of cell ν, $V^{(j)}_{\nu\ capt} = f(C^{(j)}_{\nu}, R^{(j)<100>}_{\nu})$, and the maximum volume required to capture all neighboring cells, $V^{(j)}_{\nu\ max}$
  - Calculation of the fraction of structure (j) in cell ν, $g^{(j)}_{\nu} = \min [(V^{(j)}_{\nu}-V^{(j)}_{\nu\ capt})/(V^{(j)}_{\nu\ max}-V^{(j)}_{\nu\ capt}), 1]$

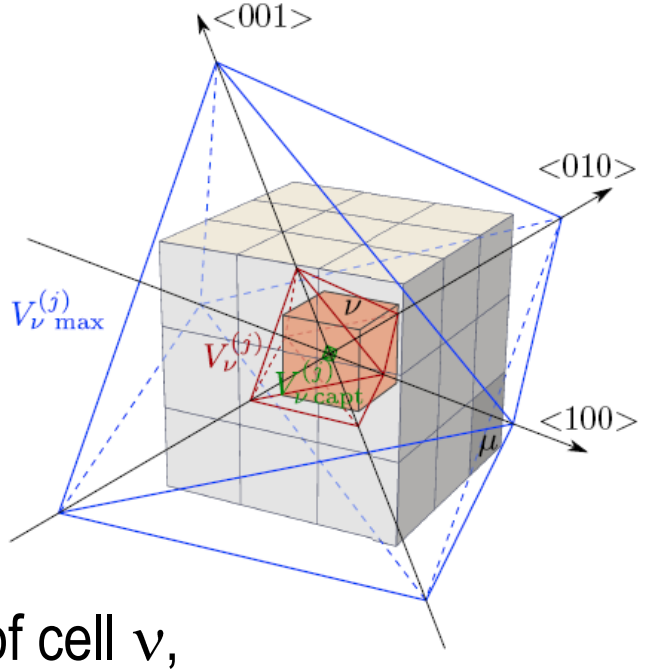

- Structure propagation to a neighboring cell μ
  - Test for $I^{(j)}_{\mu}=0$ prior to capture, test for liquid in cell μ, change to $I^{(j)}_{\mu}=1$ after capture
  - Test for the center of cell μ inside the growth shape associated with cell ν
  - Propagation of the grain $(\phi_1,\Phi,\phi_2)^{(j)}_{\mu}=(\phi_1,\Phi,\phi_2)^{(j)}_{\nu}$
  - Calculation of $C^{(j)}_{\mu}$, $R^{(j)<100>}_{\mu}$, $V^{(j)}_{\mu\ capt}$, $V^{(j)}_{\mu\ max}$ and $g^{(j)}_{\mu}$

- Nucleation kinetics
  - Gaussian distribution of nucleation sites for a structure (j) as a function of the undercooling
    - Random selection of cells for assignment of nucleation sites
    - Random selection of Euler angles (ϕ_1,Φ,ϕ_2) for each nucleation site
- Growth kinetics
  - Phenomenological growth kinetics model for the shape associated to the cells
    - Ivantsov solution and marginal stability (dendrite tip kinetics)
    - Extention to account for the fluid flow intensity and direction with respect to the growth directions (assumed <100> for cubic materials)
- Mushy zone solidification
  - Tabulation of thermodynamic properties for each phase in structure (j) assuming a given solidification path (phase volume fraction, phase composition and phase enthalpy as a function of temperature and the average composition)

ESRF directional set-up

Direct macro

- Experimental set-up at the European Synchrotron Radiation Facility (ESRF, beam line ID19)

Sample dimension:
37 mm x 6 mm x **200 µm**

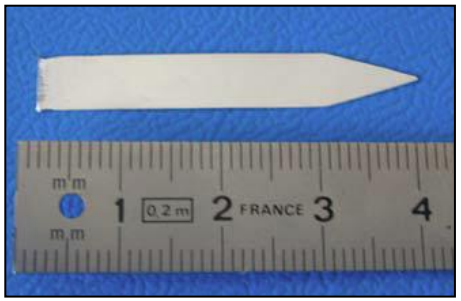

Vacuum chamber

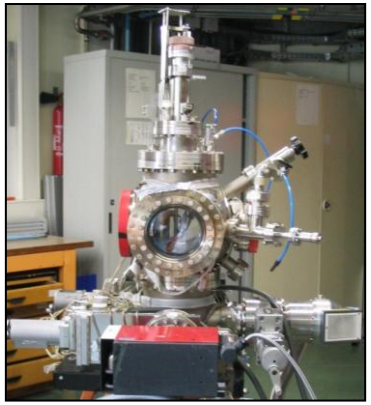

Monochromatic beam

~ 13.5 keV

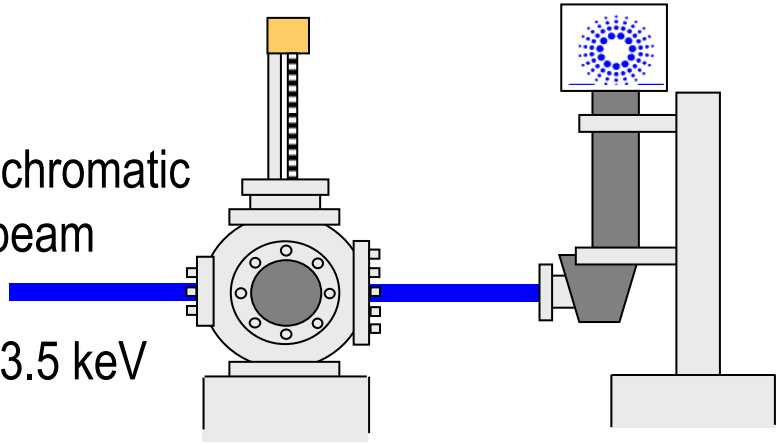

Vacuum chamber

FReLoN camera

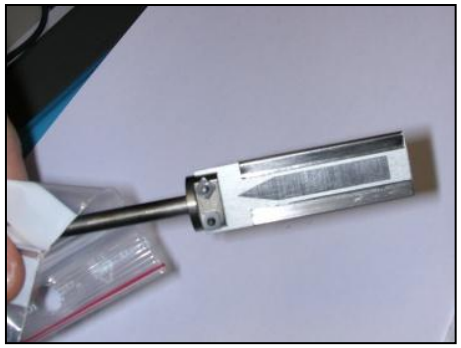

Soft crucible :
graphite foils +
Mo frame and clips

Bridgman Furnace

Field of view : 15 x 6 mm^2
Pixel size : 7.46 µm
1 frame / 3 seconds

In situ real-time X-Ray imaging
of phases in Al - 3.5 wt% Ni

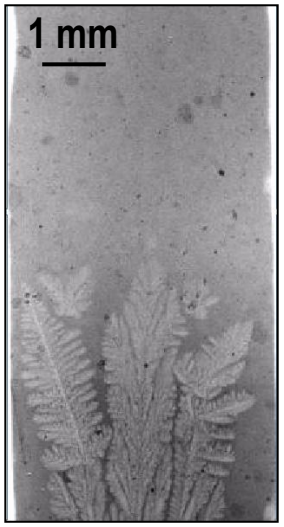

H. Nguyen-Thi et al. 2007 Metall.Mater. Trans. A 38 1458

In-situ imaging of solidification — Direct macro

- Directional solidification of Al - 3.5 wt% Ni

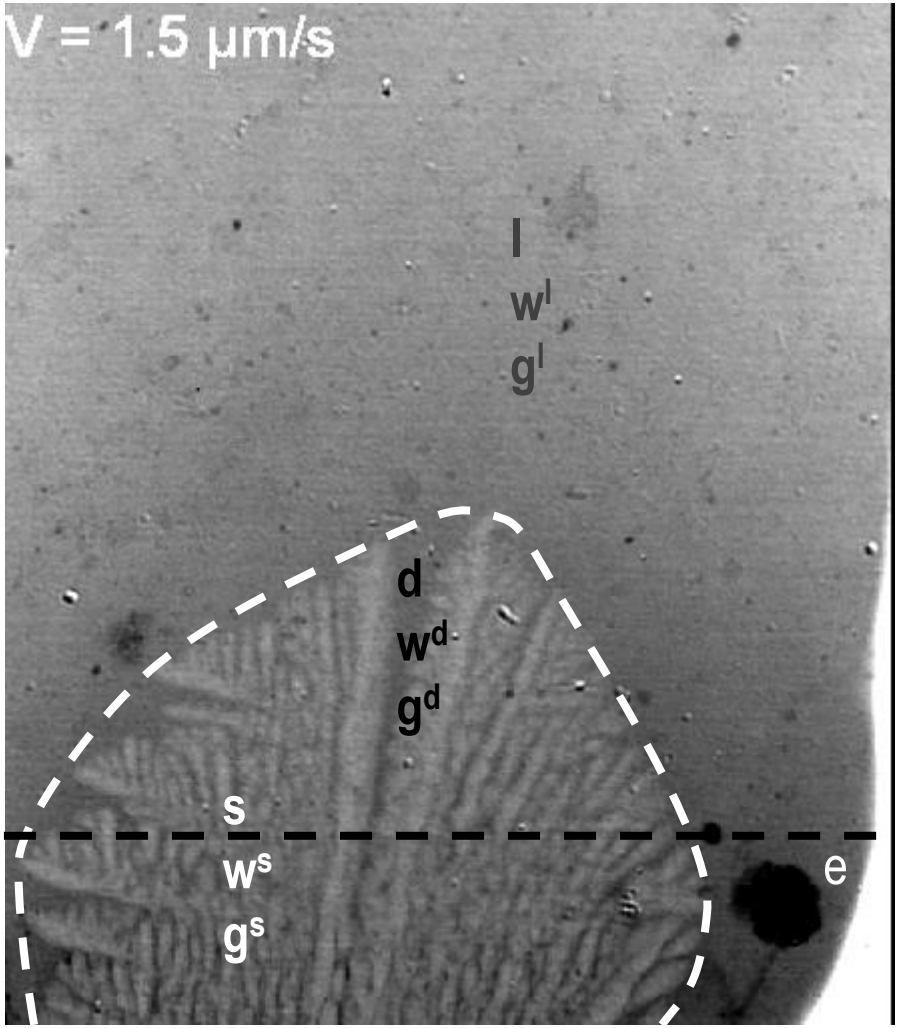

Al - 3.5 wt% Ni,
G = 20 K/cm, V = 1.5⟶15 µm/s
X-Ray radiography

- *Dendritic grain*
  - envelope delimited by the dendrite tips
  - mixture of dendritic Al-rich solid **s** plus interdendritic liquid **d** or interdendritic eutectic
  - growth in extradendritic liquid phase **l**, stopped by the extradendritic eutectic **e**
- *Segregation of elements at s/l interface*
  - average composition $\mathbf{w^s}$, $\mathbf{w^d}$, $\mathbf{w^l}$
  - average fraction of phases $\mathbf{g^s}$, $\mathbf{g^d}$, $\mathbf{g^l}$
- *Dendritic-to-eutectic transition (DET)* 1.5 µm/s
- *Columnar-to-equiaxed transition (CET)* upon velocity jump at 15 µm/s

- Distribution of inter- and intra-granular eutectic?
  Role of dendritic grain structure on eutectic distribution?

- Measured parameters as inputs for simulations
  - Characterization of the nucleation event for each grain: position x_i, y_i + orientation θ_i

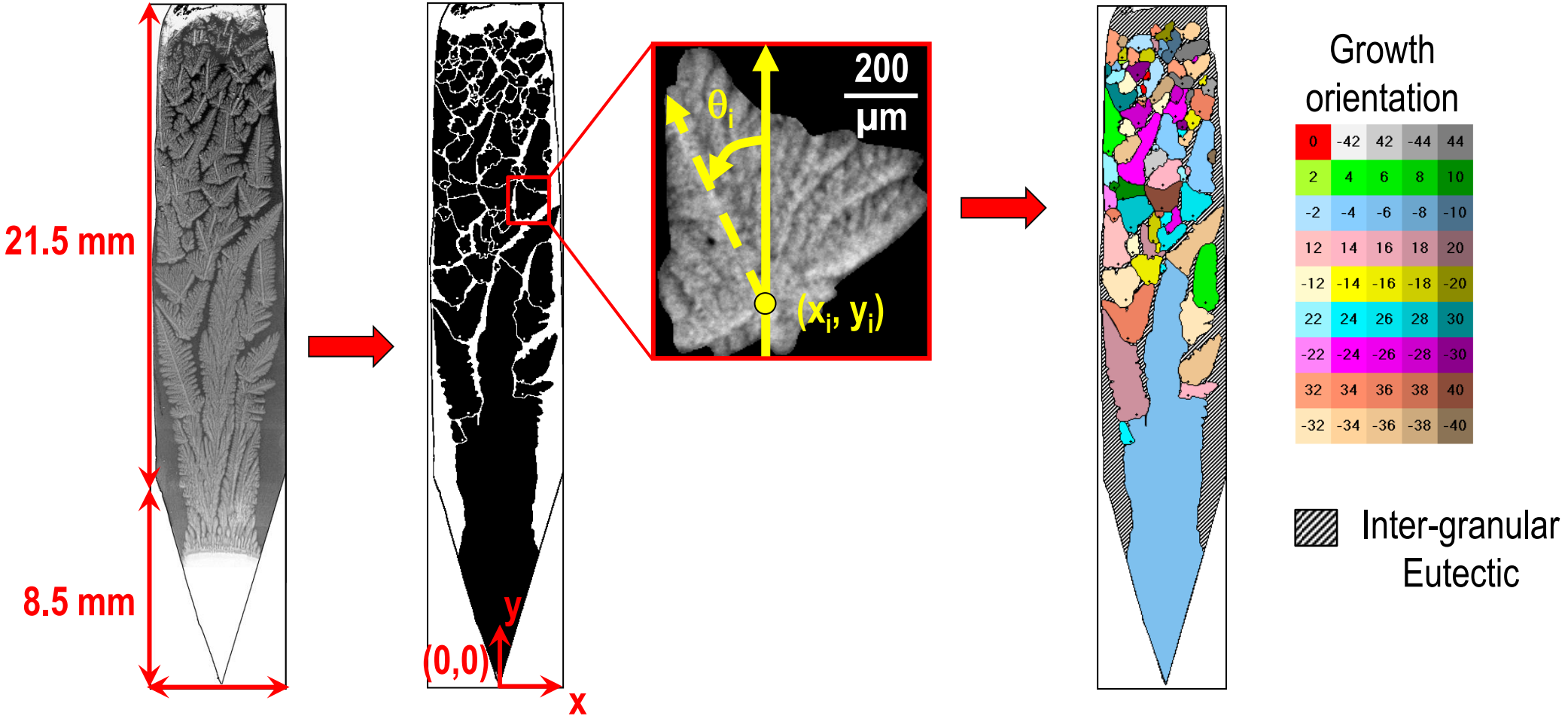

  - Measurement of the average dendrite arm spacing: 130 µm
  - Measurement of time evolution of the size of the mushy zone

Reinhart et al. 2012 IOP Conf. Ser.: Mater. Sci. Eng. 33 012077

CAFE simulation

Direct macro

- Observation
- Grain structure
- Composition
- Eutectic

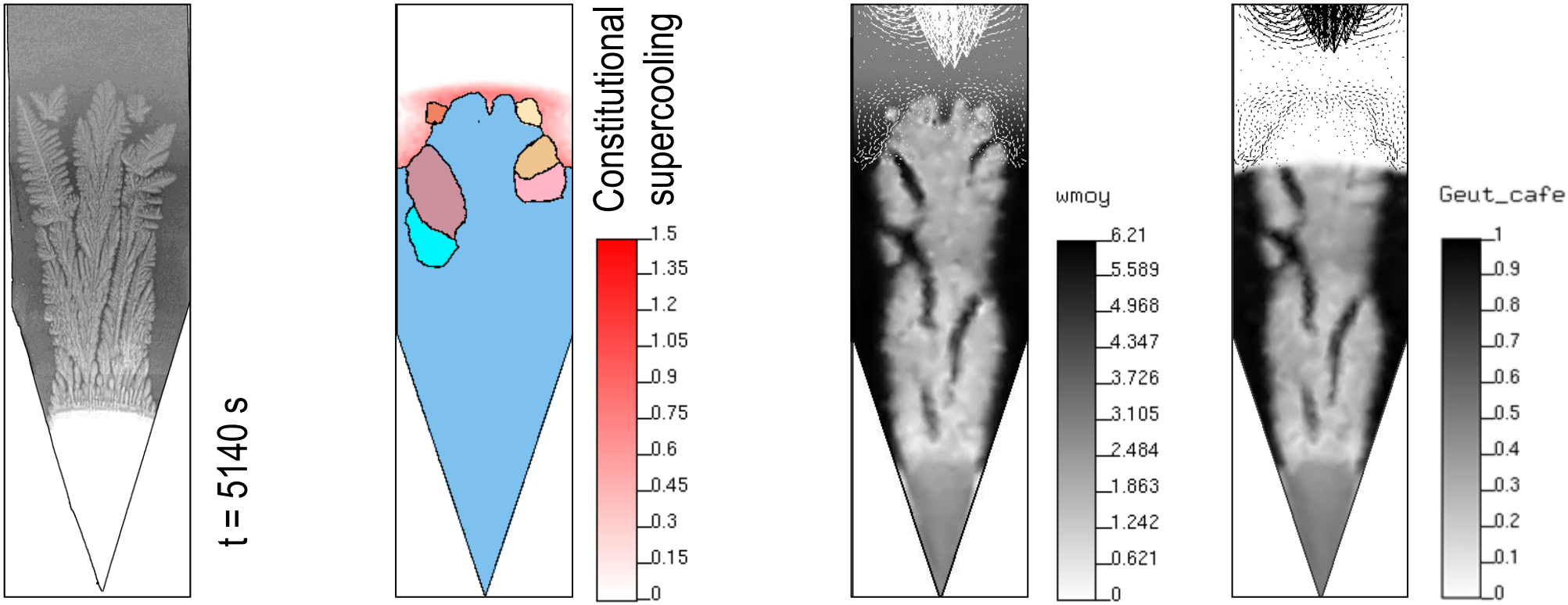

- The interaction of the liquid flow with the structure is computed
- The segregation pattern is linked with the grain structure and the eutectic fractions
- The Columnar-to-Equiaxed Transition (CET) is reproduced
- Inter- and intra-granular eutectics are partly distinguished
- Dendritic-to-eutectic transition is qualitatively retrieved

Limitations

- To be improved…
  - **Direct tracking of the primary eutectic structure** is missing to reach better comparison with in-situ observation.
  - **3D effects can not be fully neglected**.
  - **Assessment of nucleation undercooling and better measurements of the temperature fields** would permit improved comparison.
  - **Measurements of the composition field and the liquid velocity fields** are missing.
  - Coupling with thermo-mechanics is required to give access to **shrinkage** and deformation.
  - **Sedimentation of the grains** is not accounted for.

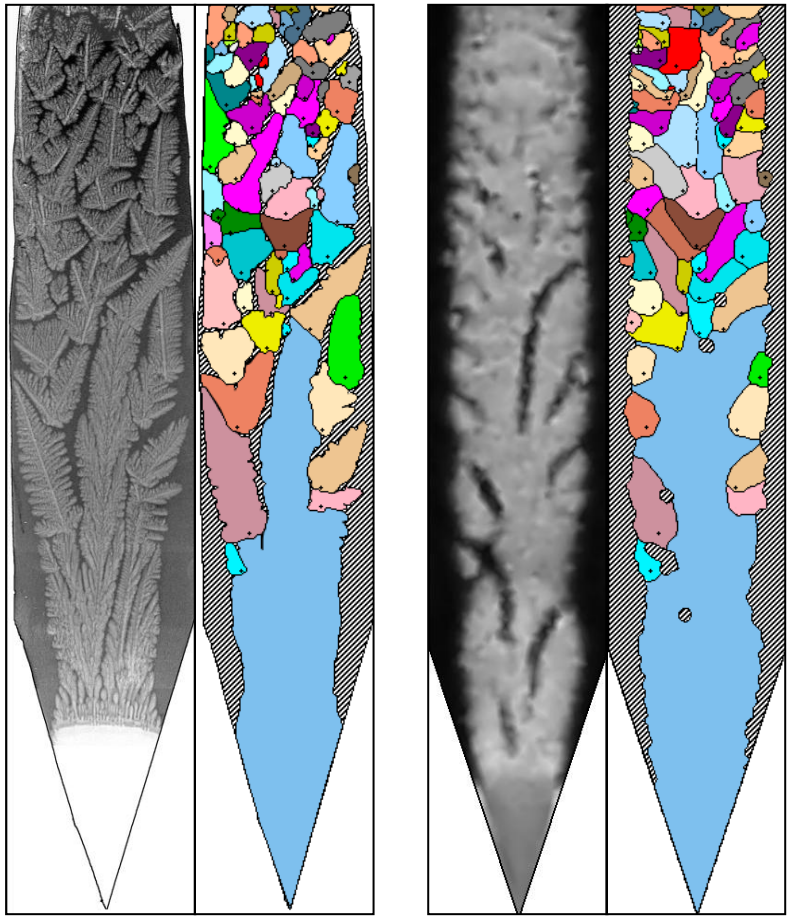

Exp. Sim.

Exp: Eutectic phase

Simu: Eutectic fraction > 0.9

AlSi in cylindrical mold – Grains

Direct macro

- Parallel FE solver
  - Coupled solutions for heat, solute and fluid flows
  - 3D automatic remeshing
- Parallel CA solver
  - Dynamic allocation of CA grid based on FE mesh
  - Nucleation and growth of dendritic and eutectic
- Coupling between the CA and FE solvers
  - Computation of mushy zone fraction from CA cells
  - Conversion of average enthalpy at FE nodes
- Coupling with thermodynamic
  - Tabulated enthalpies as a function of temperature
  - Tabulated solidification path (ThermoCalc+PBIN)

CET in Al-Si (diameter 7 cm)

Competition between columnar and equiaxed structures

Carozzani et al. 2012 MSMSE 20 015010

AlSi in cylindrical mold – Temp. Direct macro

- Retrieves well the occurrence of a recalescence recorded at 140 mm in the equiaxed region and the inflection recorded at 100 and 120 mm (validation of the coupling for heat flow together with the growth undercooling)

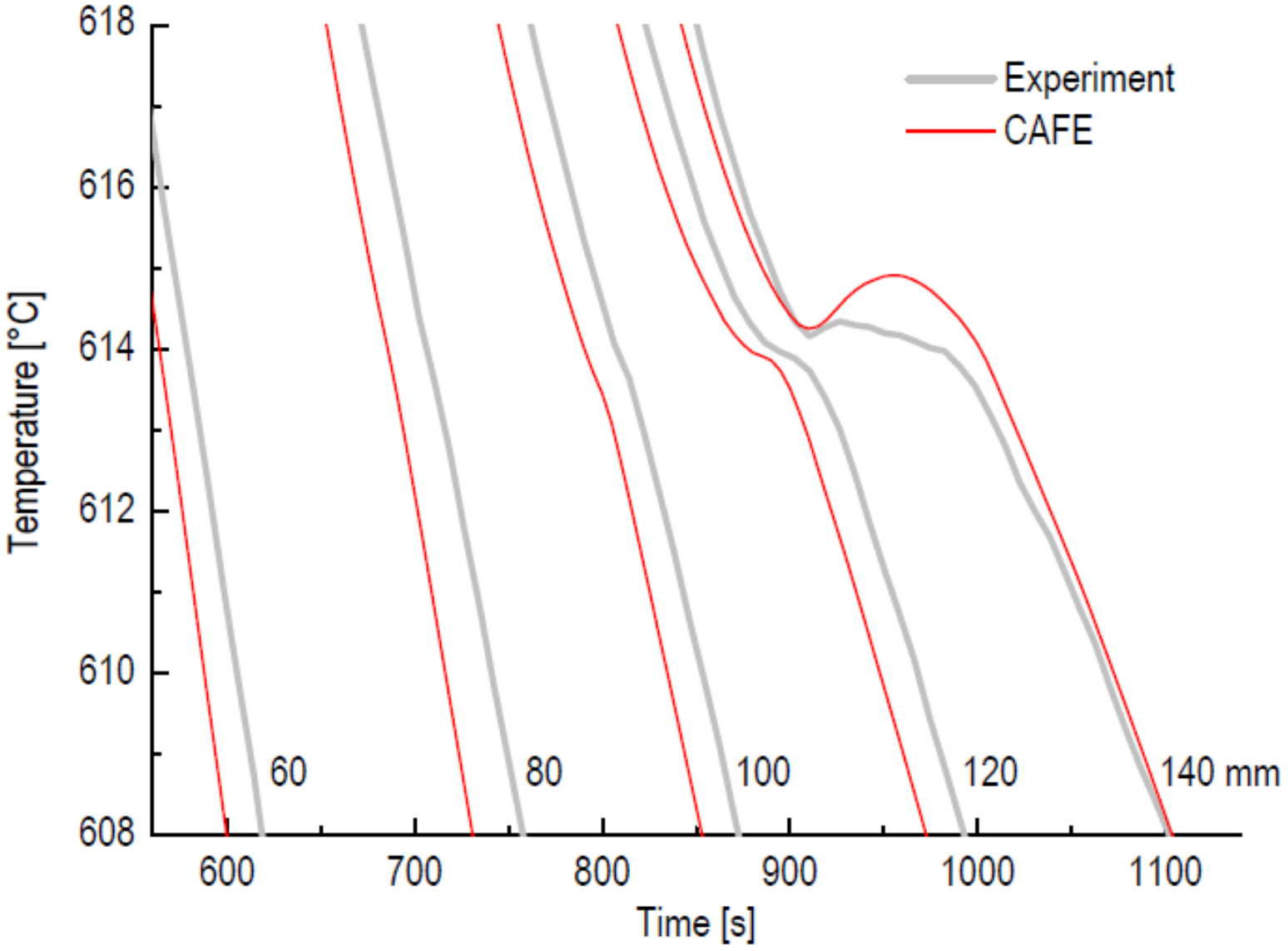

SnPb in rectangular cavity – Set-up Direct macro

- Developed at Institut National Polytechnique (Grenoble, FR)
  Hachani et al. 2012 Int. J. Heat and Mass Transfer 55 1986
- Inspired from Hebditch and Hunt 1974 Metall. Trans. 5 1557
  - Left-hand-side (LHS) and right-hand-side (RHS) heat exchangers with independent control of the time evolution of the temperature
  - 100x60x10 mm^3 geometry
  - Sn - 3 wt% Pb alloy
  - T_{LHS}-T_{RHS} = 40 °C
  - Cooling rate = -0.03 °C/s
  - Thermocouples

    10 columns, 5 rows
  - Positions from LHS (mm)

L21	L24	L27	L30
5	35	65	95

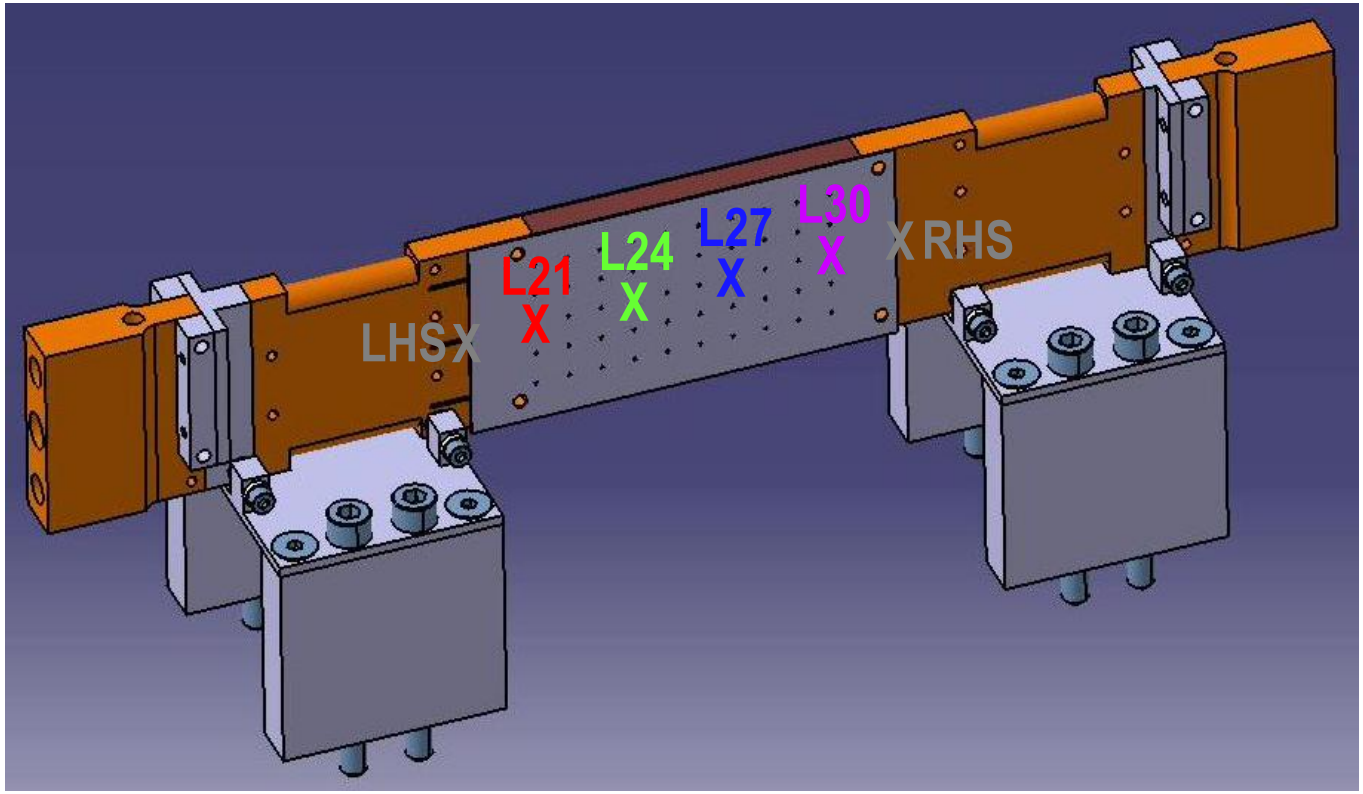

SnPb in rectangular cavity – Meas. Direct macro

- Accurate measurements with control temperature at LHS and RHS boundaries
- Possibility to extract time evolution of temperature maps

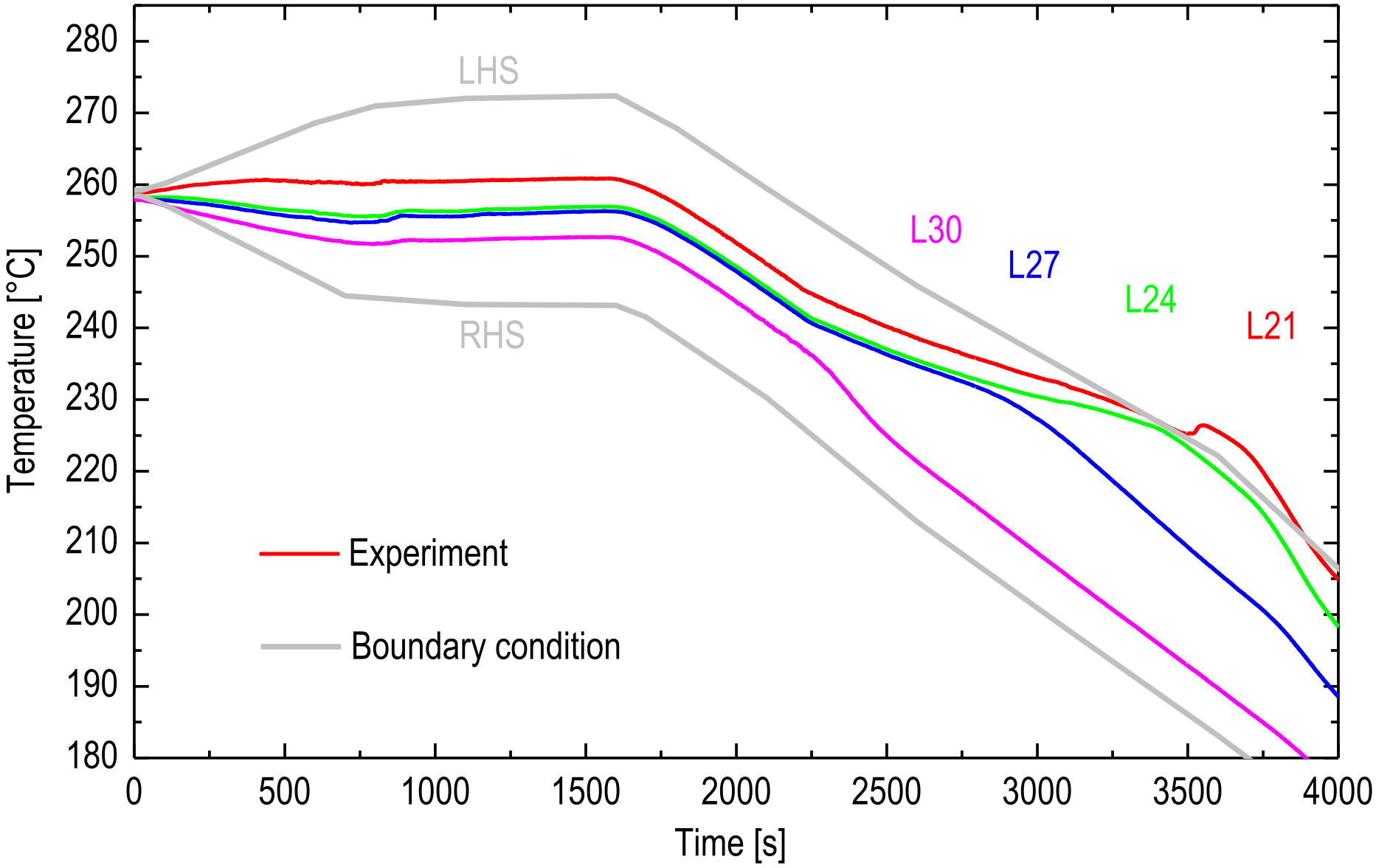

SnPb solidification paths – Tab. Direct macro

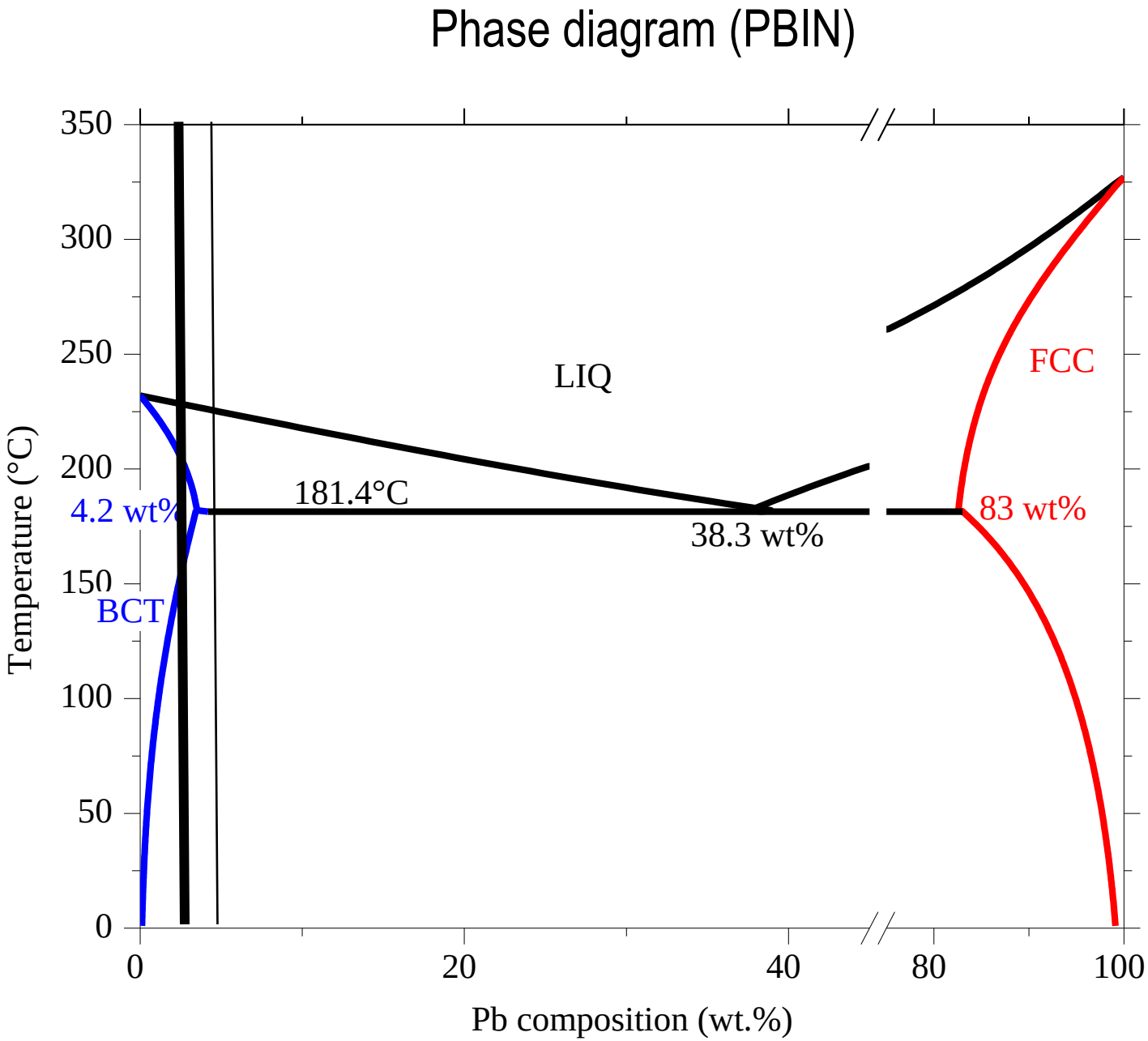

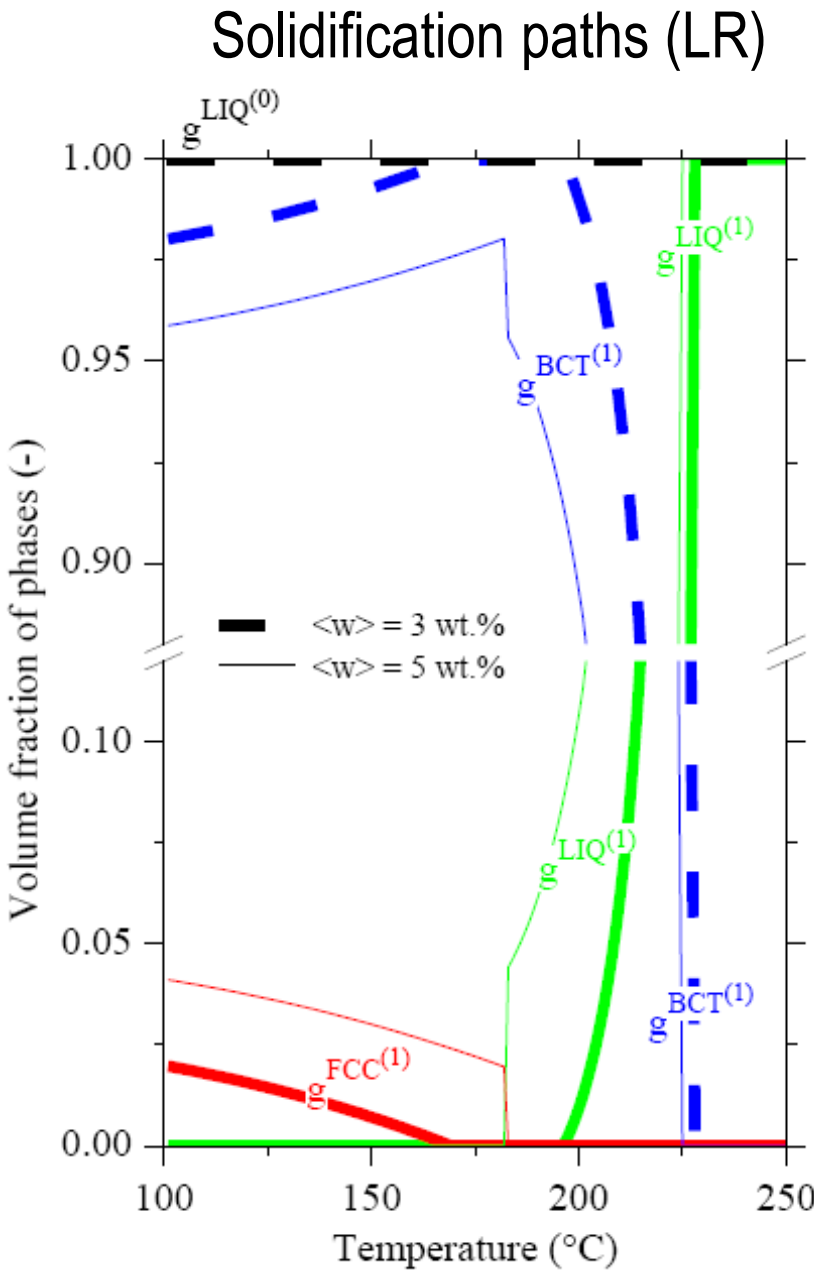

SnPb properties – Tab.

Direct macro

Phase composition

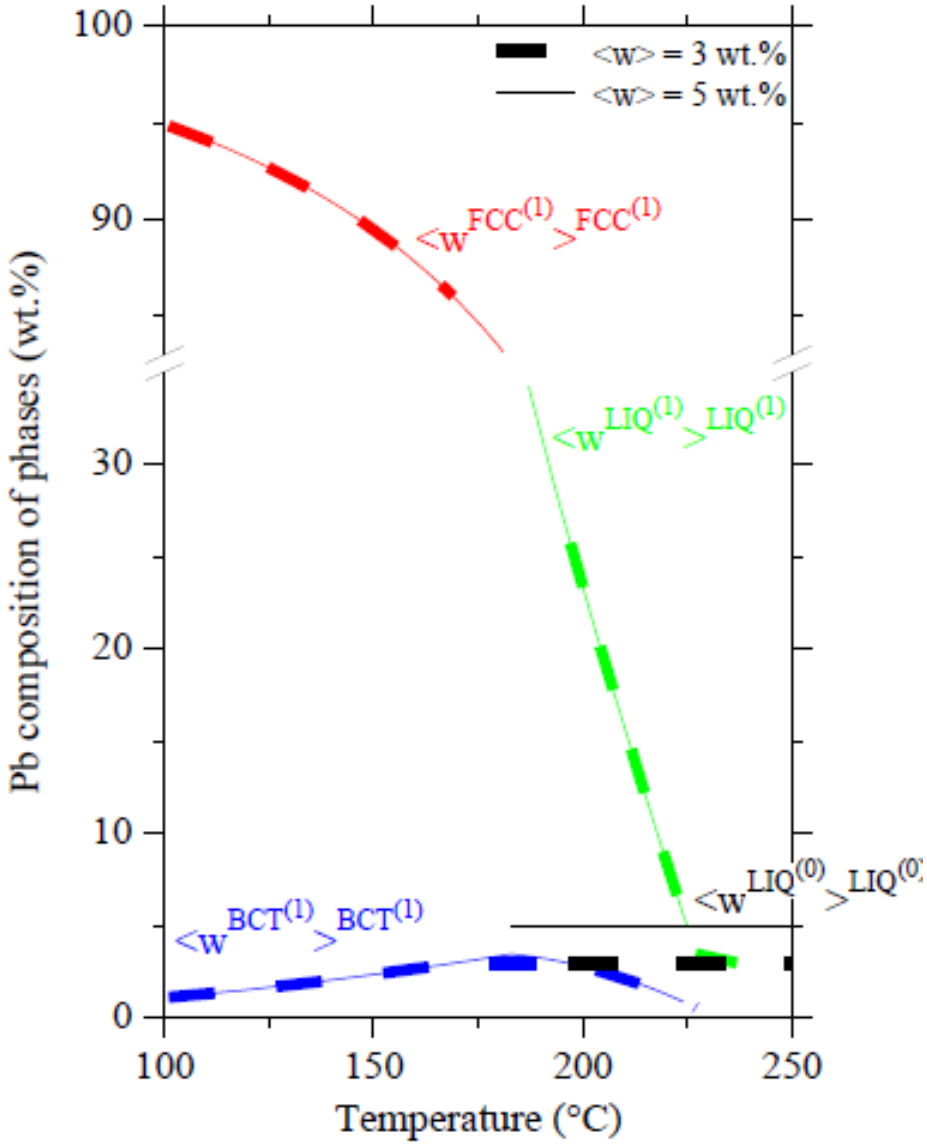

Phase enthalpy

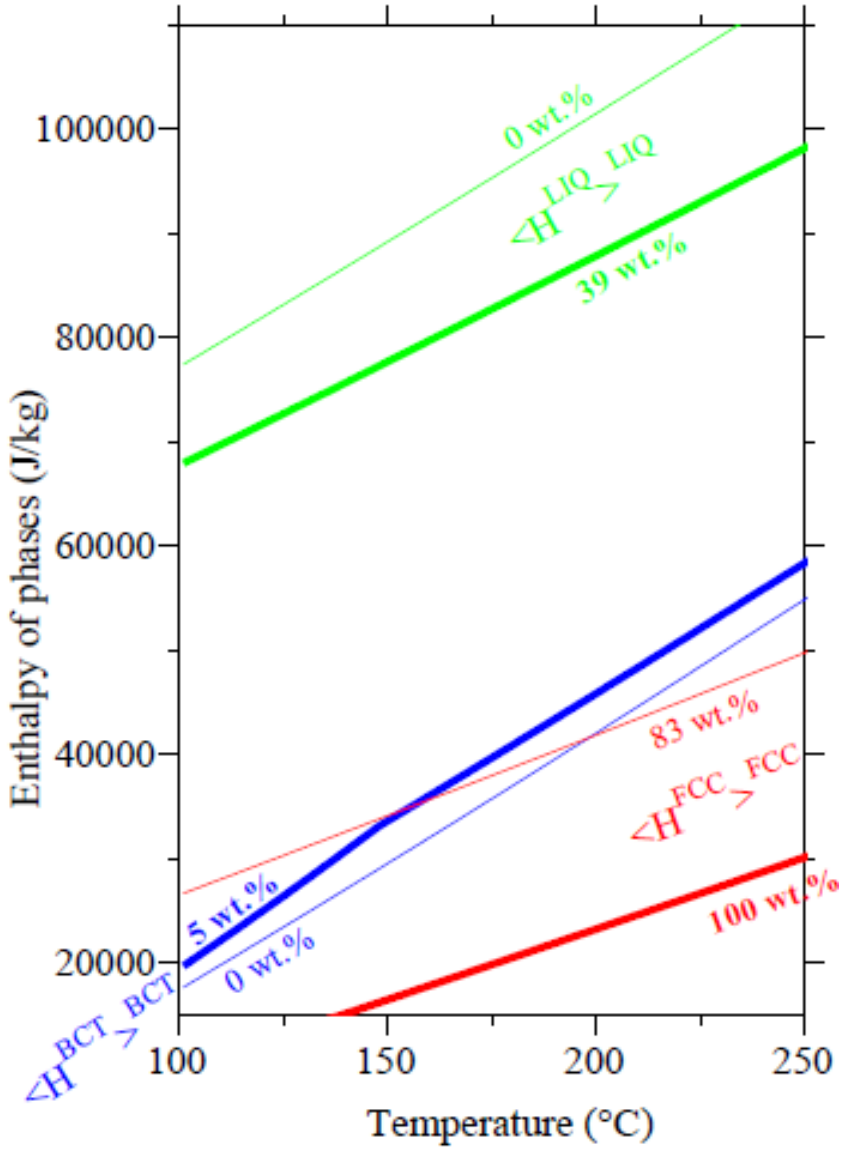

SnPb in rectangular cavity – Flows

Direct macro

- CA grid: 200 μm (7'500'000 cells)
- FE mesh:
  - Initial: 1'200 μm (76'000 nodes)
  - Final: [780-1'200] μm
- Time step: 0.1 s
- Cluster: 64 processors
- CPU time: 4 days

- Nucleation sites
  - RHS: $n=5\cdot10^4$ m^{-2}, $\Delta T_a=1.5$ °C, $\Delta T_\sigma=0.5$ °C
  - Volume: $n=10^7$ m^{-3}, $\Delta T_a=5$ °C, $\Delta T_\sigma=0.5$ °C

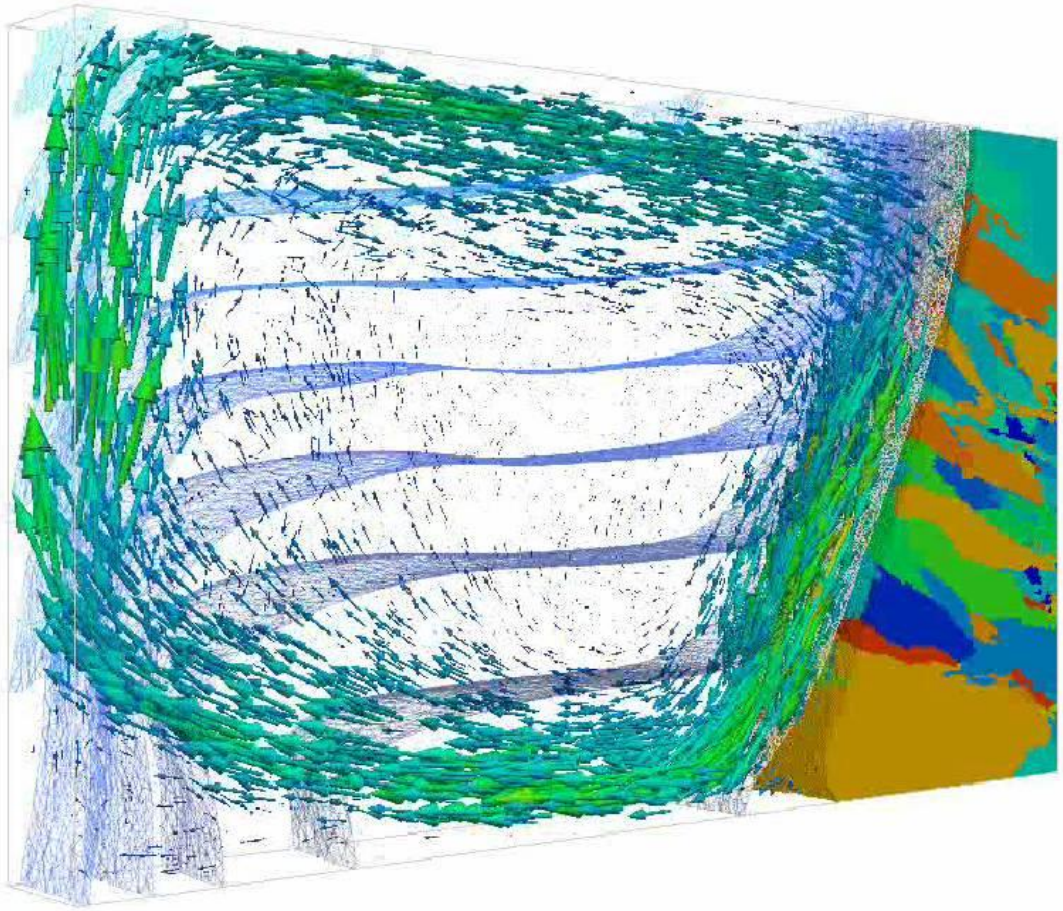

Isothermal surfaces every 2°C
Flow (max arrow 2.5 cm s^{-1})
(Time acceleration x100)

T. Carozzani et al. 2012
Metallurgical and Materials
Transactions in press.

SnPb in rectangular cavity – Segreg. Direct macro

Radiography

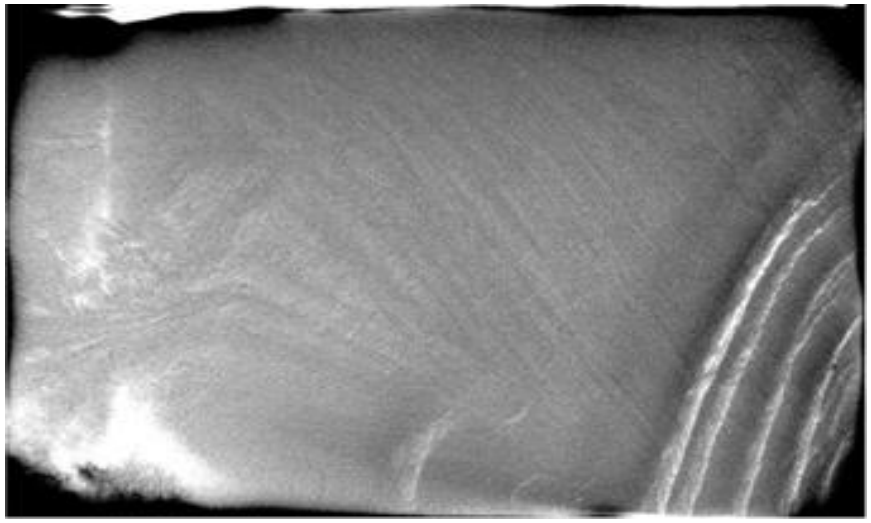

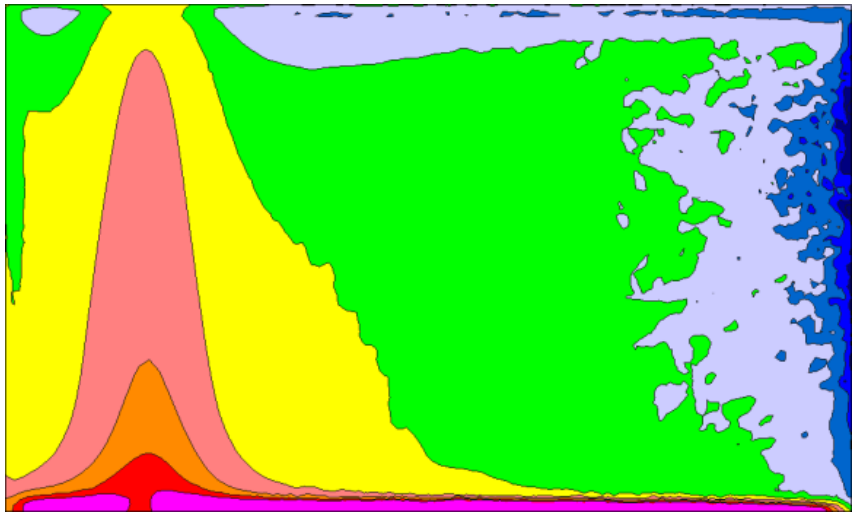

3D FE simulation

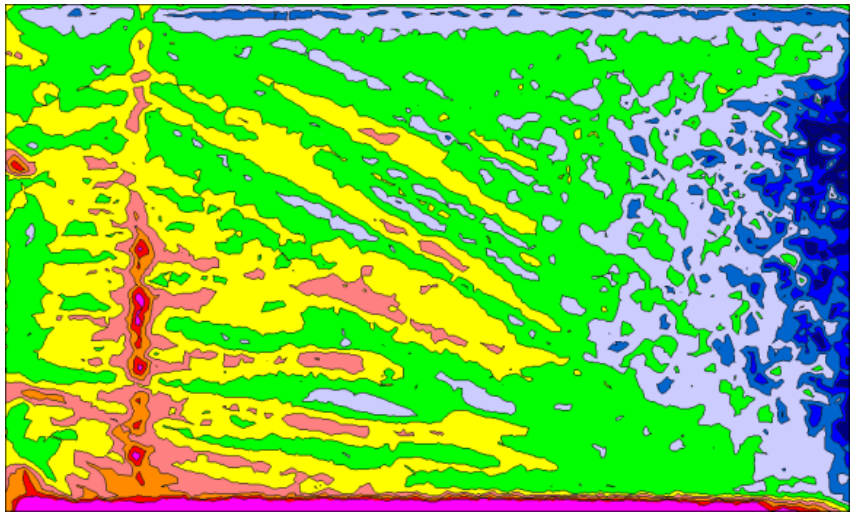

3D CAFE simulated segregation map

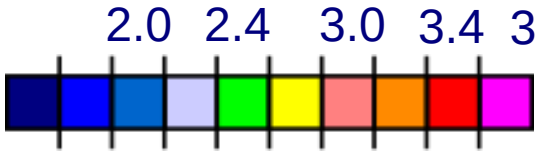

SnPb in rectangular cavity – Grains **Direct macro**

Casting surface

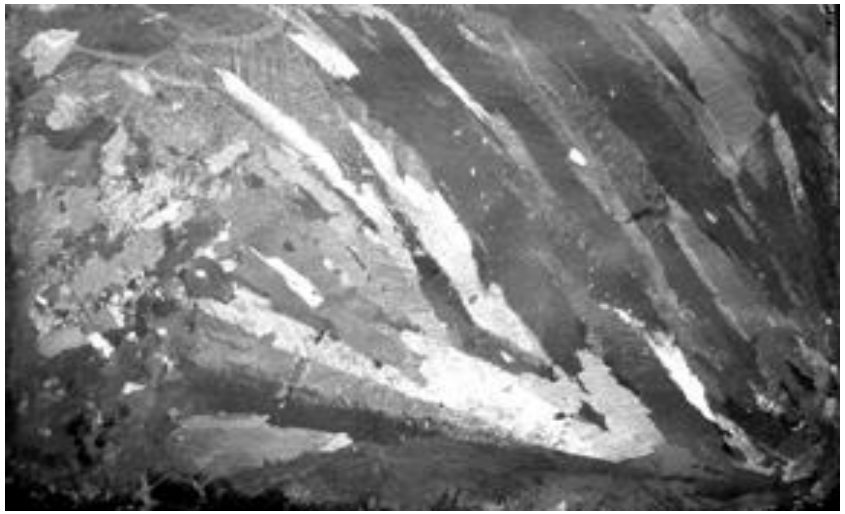

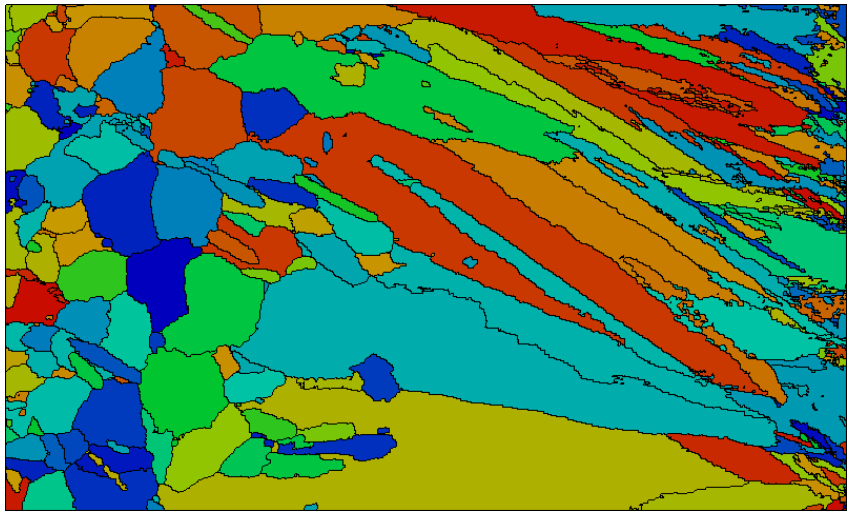

CAFE V_I

$n = 10^8\ m^{-3}$

$\Delta T_a = 3.5°C$

$\Delta T_\sigma = 0.5\ °C$

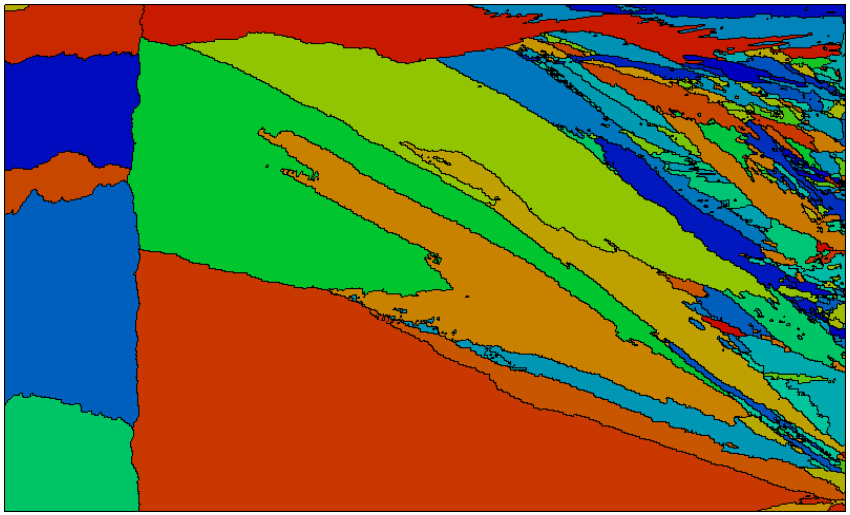

CAFE V_II

$n = 10^7\ m^{-3}$

$\Delta T_a = 5°C$

$\Delta T_\sigma = 0.5\ °C$

SnPb in rectangular cavity – Temp. Direct macro

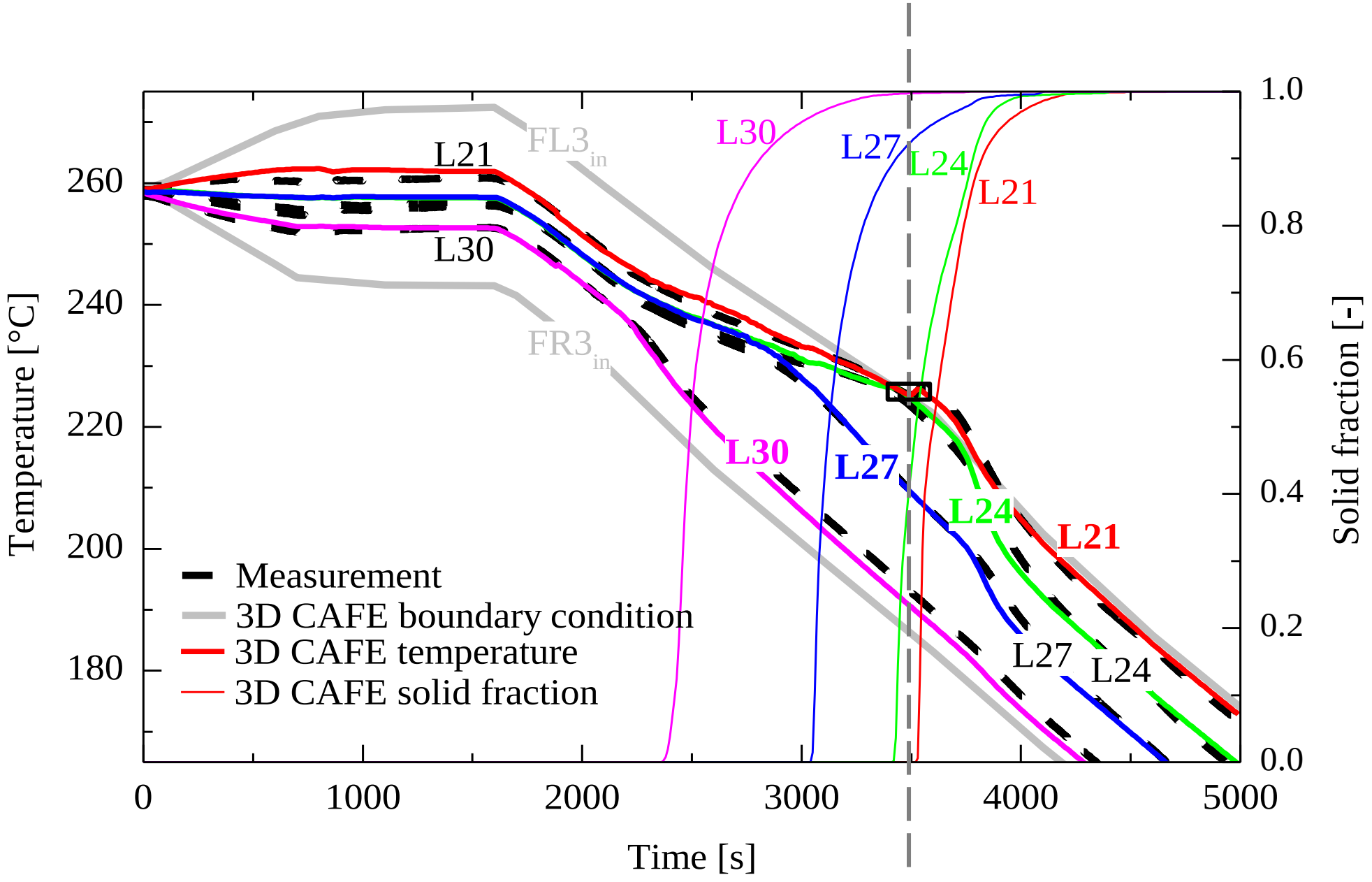

SnPb in rectangular cavity

Direct macro

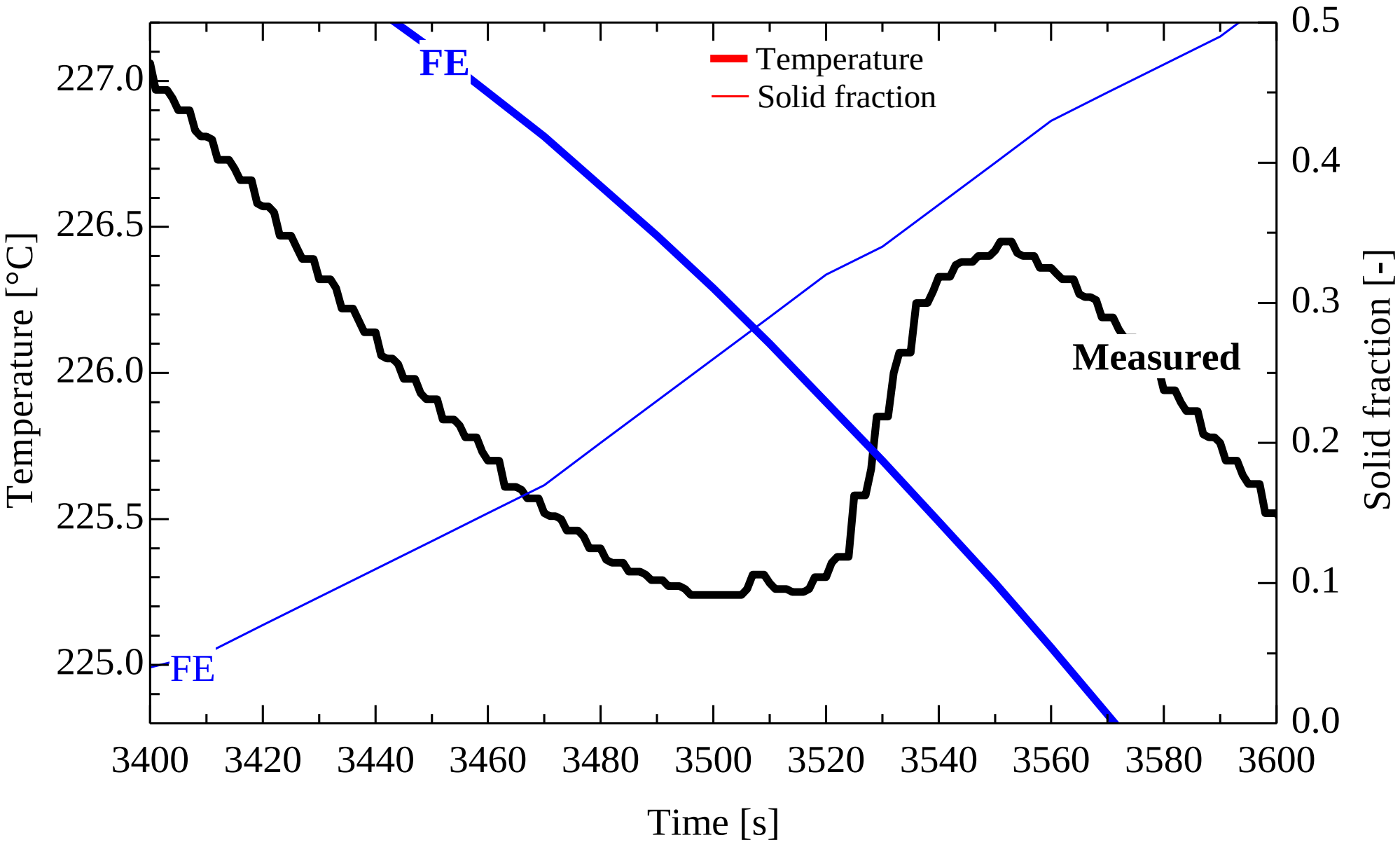

SnPb in rectangular cavity

Direct macro

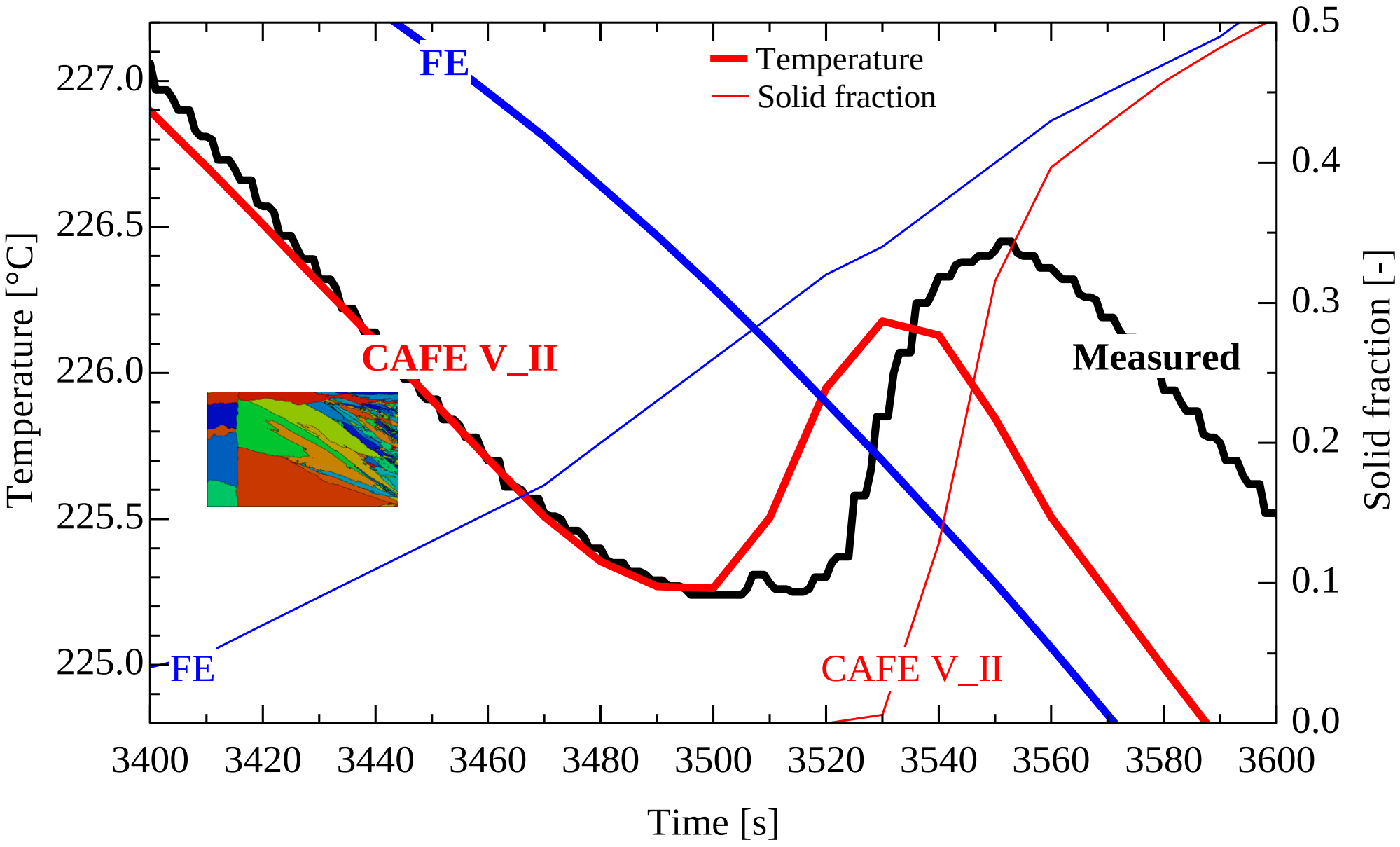

SnPb in rectangular cavity

Direct macro

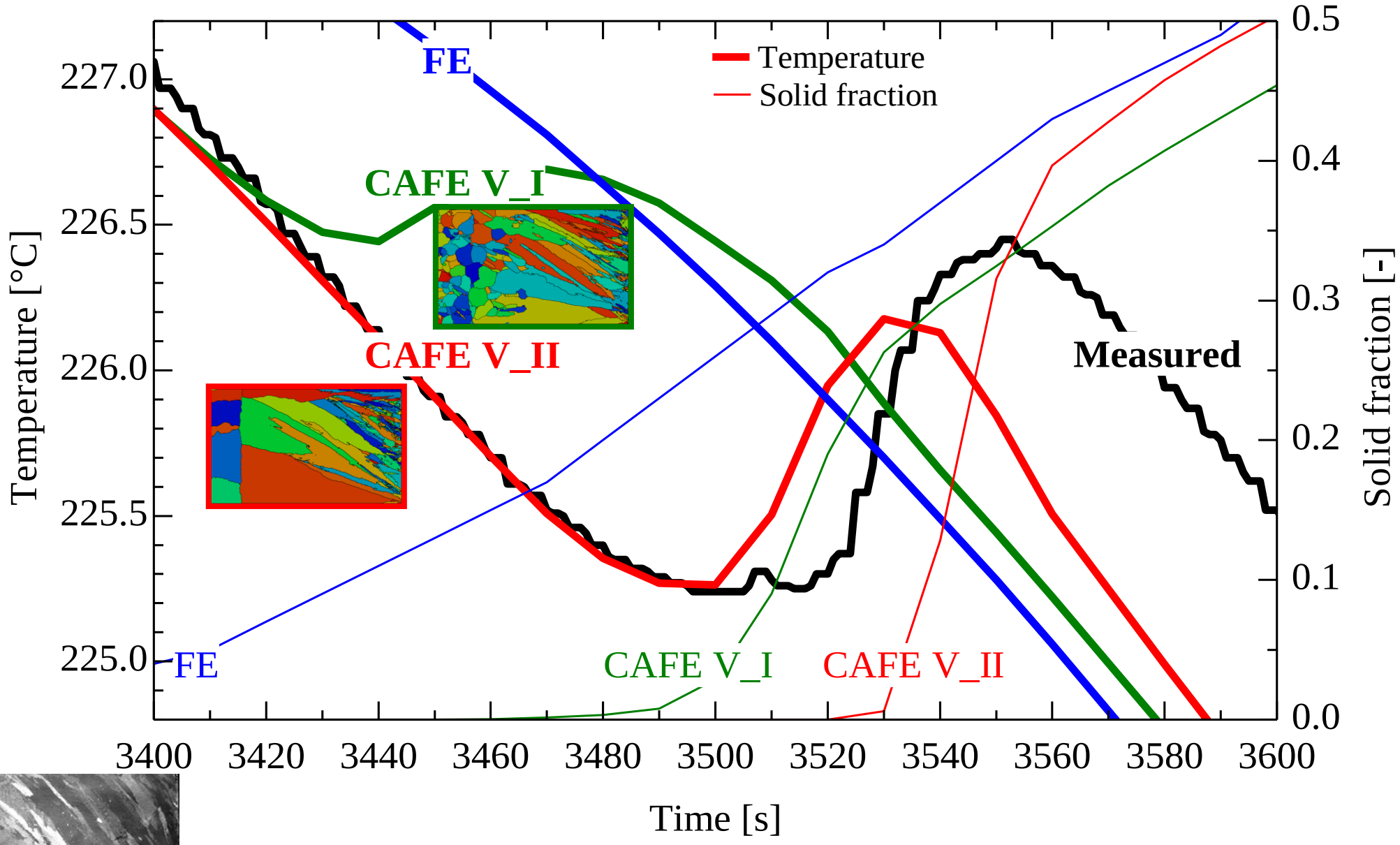

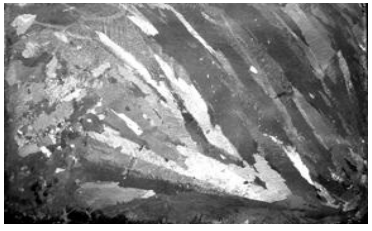

Improvement of nucleation kinetics required. Fragmentation?

Perspectives

- Main scientific problems
  - Nucleation laws not well characterized
  - Fragmentation of mushy zone known as a source of crystals, but not understood
  - Upscaling: modeling of a unique single grain with a direct microscopic method (e.g., phase field) for improving macroscopic models (e.g., CAFE)
  - Coupling with deformation of the mushy zone during the formation of the solidification structure required (hot tear, shrinkage porosity, macrosegregation)
  - Links with subsequent thermomechanical processing steps while inheriting from the solidification structure (e.g., PFZ formed upon homogenization heat treatment)
  - Measurement of missing properties (e.g., interfacial energy and its anisotropy, mobilities)
- Direct simulation of structures
  - Need for more dedicated experiments with well controlled boundary conditions, with
  - in-situ and post-mortem characterizations, to be compared with
  - more integrated modeling with multiple scale physics and thermodynamic properties.